

ARTICLE

Coevolution promotes the coexistence of Tasmanian devils and a fatal, transmissible cancer

Dale T. Clement,^{1,*} Dylan G. Gallinson,² Rodrigo K. Hamede,^{3,4} Menna E. Jones,³ Mark J. Margres,² Hamish McCallum⁵ and Andrew Storfer^{6,*}

¹Department of Biology, Wake Forest University, Winston-Salem, NC, 27109, USA, ²Department of Integrative Biology, University of South Florida, Tampa, FL, 33620, USA, ³School of Natural Sciences, University of Tasmania, Hobart, TAS, 7001, Australia, ⁴CANECEV: Centre de Recherches Ecologiques et Evolutives sur le Cancer, Montpellier, 34394, France, ⁵Centre for Planetary Health and Food Security, Griffith University, Nathan Campus, Nathan, Queensland, 4111, Australia and ⁶School of Biological Sciences, Washington State University, Pullman, WA, 99164, USA

*Corresponding authors: clemend@wfu.edu, astorfer@wsu.edu

Abstract

Emerging infectious diseases threaten natural populations, and data-driven modeling is critical for predicting population dynamics. Despite the importance of integrating ecology and evolution in models of host-pathogen dynamics, there are few wild populations for which long-term ecological datasets have been coupled with genome-scale data. Tasmanian devil (*Sarcophilus harrisii*) populations have declined range-wide due to devil facial tumor disease (DFTD), a fatal transmissible cancer. Although early ecological models predicted imminent devil extinction, diseased devil populations persist at low densities, and recent ecological models predict long-term devil persistence. Substantial evidence supports evolution of both devils and DFTD, suggesting coevolution may also influence continued devil persistence. Thus, we developed an individual-based, eco-evolutionary model of devil-DFTD coevolution parameterized with nearly two decades of devil demography, DFTD epidemiology, and genome-wide association studies. We characterized potential devil-DFTD coevolutionary outcomes and predicted the effects of coevolution on devil persistence and devil-DFTD coexistence. We found a high probability of devil persistence over 50 devil generations (100 years) and a higher likelihood of devil-DFTD coexistence, with greater devil recovery, than predicted by previous ecological models. These novel results add to growing evidence for long-term devil persistence and highlight the importance of eco-evolutionary modeling for emerging infectious diseases.

Key words: Tasmanian devil, eco-evolutionary dynamics, host-pathogen coevolution, disease ecology, individual-based model, quantitative genetics

Introduction

Emerging infectious diseases (EIDs) are a leading threat to natural populations. EIDs have directly caused the extinction of many species (Fisher et al. 2012) and contributed to the decline of numerous others (De Castro and Bolker 2005b; Jones et al. 2008). The epidemiological outcome of an EID, ranging from local host extirpation to pathogen extirpation to forms of coexistence and disease endemism, results from a complex interplay of both ecological and coevolutionary processes (McKnight et al. 2017; Vander Wal et al. 2014a). By creating *in silico* experiments that would be impossible to conduct in the field or lab, data-driven modeling plays an important role in predicting how ecology and coevolution interact to drive the outcomes of EIDs. Evolution regularly occurs on ecological timescales, particularly for pathogens (Hairston et al. 2005; Hendry and Gonzalez 2008; Hendry et al. 2018), and the study of “eco-evolutionary dynamics” over the past two decades (Post and Palkovacs 2009; Schoener 2011; Reznick et al. 2019) has facilitated efforts to combine epidemiological and coevolutionary theory (Vander Wal et al. 2014a; Boots et al. 2009; Lively 2010, 2016). However, there is still a pressing need to apply this theory to species of conservation concern (Vander Wal et al. 2014a; Smith et al. 2014; Shefferson et al. 2018; Brannelly et al. 2021).

Epidemiological theory predicts that patterns of pathogen transmission strongly affect the likelihood that an EID results in population extirpation. For many pathogens the rate of transmission decreases with host density, which leads to disease fadeout rather than host extirpation, as host populations decline over the course of an epidemic (McCallum et al. 2001). However, if pathogen transmission is independent of host density (e.g. sexually transmitted diseases, where transmission is strongly coupled with host mating behavior), the resulting frequency-dependent transmission may drive populations to extinction (De Castro and Bolker 2005a; McCallum et al. 2001). High disease-related mortality often leads to rapid population collapse during an epizootic outbreak (Vredenburg et al. 2010) or slow population decline and extinction for endemic pathogens that reduce host per-capita reproduction below replacement (Valenzuela-Sánchez et al. 2017). Notably, many high-profile EIDs responsible for mass population declines are characterized by high disease-related mortality (e.g. chytrid, Lips et al. 2006; white nose syndrome; Hoyt et al. 2021).

Rapid evolution can dramatically affect the outcome of a disease outbreak; there are many documented cases of evolution “rescuing” natural populations from disease-induced extinction (most prominently in biocontrol, e.g. the initial stages of the myxoma epizootic in Australian rabbits; reviewed in Kerr 2012). The effect of evolution depends on which traits are under selection. The evolution of host resistance (reduced susceptibility) and host tolerance (reduced disease-related mortality) are both predicted to reduce the likelihood of host extirpation. However, the evolution of resistance is predicted to decrease disease prevalence while the evolution of tolerance promotes greater disease prevalence and host-pathogen coexistence (Roy and Kirchner 2000; reviewed in Searle and Christie 2021). Though disease evolution may in some cases synergize with host evolution to promote host persistence (many highly-virulent EIDs have evolved reduced virulence during the initial disease outbreak; Bolker et al. 2010; e.g. myxoma virus, Kerr 2012), rapid coevolution of both host and pathogen may also lead to host extirpation or a long-term reduction in host abundance. For example, the phenotypic difference model, a common quantitative trait model of coevolution, assumes that a disease-related trait (usually infectivity or the fitness cost of infection) is a function of the difference between the host and pathogen genotype and predicts arm race dynamics between host resistance and pathogen transmissibility whereby the “losing” species is extirpated (Nuismer 2017). Additionally, myxoma virus evolved greater virulence in the decades following the evolution of rabbit resistance (Kerr et al. 2017, 2022) and rabbit abundance still remains well below its pre-myxoma high (Saunders et al. 2010). The effect of multivariate coevolution is even more complex, with evolutionary outcomes depending on the infection rate, background mortality, trait fitness costs, among other factors (e.g. Carval and Ferriere 2010).

Despite the growing body of theory, there are still few eco-evolutionary models of host-pathogen coevolution in species of conservation concern. Long-term ecological datasets on host-pathogen dynamics necessary to parameterize such models are rare but becoming more common (e.g., Byrne et al. 2019; Epstein et al. 2016). Given that rapid evolution frequently alters ecological dynamics (and vice versa), integrating the two data types in eco-evolutionary models is critical in an era when EIDs increasingly threaten species persistence and risk spillover to humans and livestock (Vander Wal et al. 2014b,a; Hohenlohe et al. 2019).

The Tasmanian devil (*Sarcophilus harrisii*) has experienced range-wide population declines of approximately 80% due to the devil facial tumor disease (DFTD), a fatal transmissible cancer. DFTD has generated a “natural experiment” of an EID that has spread predictably east-to-west across nearly all the devil’s known geographic range over the past ~25 years (Lazenby et al. 2018; Storfer et al. 2018; Cunningham et al. 2021). This system has been the subject of extensive, long-term collection of both ecological and genetic data (e.g., Lazenby et al. 2018; Cunningham et al. 2021; Epstein et al. 2016; Strickland et al. 2024). DFTD is transmitted by biting during frequent social interactions, such as aggregation at carcasses during scavenging and mate guarding (Hamede et al. 2008, 2013; Hamilton et al. 2019), and hence has a strong frequency-dependent component to transmission. Initial compartmental epidemiological models (McCallum et al. 2009; Beeton and McCallum 2011) predicted devil extinction due to this frequency-dependent transmission and DFTD’s high virulence.

However, all continuously-distributed diseased devil populations have persisted at low-to-medium densities (Lazenby et al. 2018) and more recent models predict continued devil persistence in the majority of scenarios (Wells et al. 2019; Siska et al. 2018), likely because most infected individuals survive to breed in the next breeding season with no vertical transmission to offspring (Wells et al. 2017; Lazenby et al. 2018). Moreover, these models are based only on ecological mark-recapture data. Evidence of evolution in both devils (Epstein et al. 2016; Fraik et al. 2020; Stahlke et al. 2021) and tumors (Patton et al. 2020; Kwon et al. 2020; Stammnitz et al. 2023) suggests rapid evolution could affect devil persistence. Devil genetic variation explains a significant proportion of phenotypic variance in survival after infection (Margres et al. 2018) and infection status (Margres et al. 2018; Strickland et al. 2024). Time series analyses of devil populations pre- and post-DFTD emergence show evidence of rapid evolutionary responses to selection in genomic regions containing immune-related genes (Epstein et al. 2016; Hubert et al. 2018; Stahlke et al. 2021). DFTD also has evolved into four genetically-distinct lineages (Patton et al. 2020; Kwon et al. 2020; Stammnitz et al. 2023) and shown local variation in tumor genetic diversity over time (Hamede et al. 2023). DFTD’s effective reproduction rate R_e – equivalent to transmission – declined from 3.5 during the exponential growth phase to ~1, or replacement, at present, suggesting the potential

evolution of DFTD toward endemism (Patton et al. 2020). Gallinson et al. (2024) found that the interaction between devil and tumor genomes explained a significant proportion of variation in force of infection (measured by proxy as the number of days a susceptible individual takes to become infected with DFTD), and identified devil and tumor genes associated with this variation. Taken together, these studies provide substantial evidence suggesting devil-DFTD coevolution in multiple disease-related traits.

However, not all traits may be as likely to evolve and it is still unclear how coevolution in different traits will impact long-term devil persistence. We expect strong coevolution between devil resistance to infection and DFTD transmissibility, as these traits have substantial underlying genetic variation (Margres et al. 2018; Gallinson et al. 2024; Strickland et al. 2024). Similarly, genetic variation in devil survival indicates the possibility for evolution of increased devil tolerance (Margres et al. 2018), though no empirical study has yet examined among lineage variation in DFTD virulence. If coevolution of DFTD virulence and devil tolerance is present, the expected outcome would be lower devil mortality and a substantial, positive effect on devil persistence and devil-DFTD coexistence (Bolker et al. 2010; Berngruber et al. 2013). Coevolution of host resistance and pathogen transmissibility, on the other hand, could lead to arms race dynamics, the outcome of which would depend on the relative rates of host and pathogen evolution (for example, if coevolution follows the phenotypic difference model; Nuismer 2017). Given the decline in DFTD transmission toward replacement, it is possible an arms race dynamic would favor devils (Patton et al. 2020; Hamede et al. 2023).

Thus it is necessary to develop an eco-evolutionary model to investigate the consequences of evolutionary dynamics for long-term devil-DFTD population dynamics and we have a unique combination of long-term mark recapture data and genomic analyses that make it feasible to parameterize such a model. Herein, we present one of the first studies to model the effect of rapid coevolution on population extirpation risk due to an EID. We ask three questions: 1) In which traits does devil-DFTD coevolution result in patterns of life history, infection, and evolution consistent with empirical data? 2) How does coevolution affect the probability of devil persistence and devil-DFTD coexistence relative to a non-evolving population? 3) In which traits is coevolution most important for driving devil persistence and devil-DFTD coexistence? To answer these questions, we developed an individual-based, eco-coevolutionary model of devil-DFTD dynamics with coevolution in three pairs of DFTD and devil traits: 1) the probability of tumor transmission and devil resistance to infection; 2) tumor growth rate on an infected individual and devil resistance to growth; 3) tumor virulence and devil tolerance (following the definitions of Råberg et al. 2009). Via model parameterization, we first predict which traits are most likely to be coevolving and, second, we use simulations to test how- and in which traits- coevolution affects the probability of devil and DFTD persistence to 50 generations (100 years; following Wells et al. 2019).

Methods

Model Description

We present an individual-based eco-evolutionary model of devil population and DFTD epidemiological dynamics with discrete, weekly timesteps. DFTD epidemiology follows a susceptible-exposed-infected (SEI) framework. The infected class is structured by tumor size, with larger tumors having a higher probability of transmission and causing higher mortality than smaller tumors. We focus on coevolution in three “realized” disease-related traits: 1. The realized resistance of susceptible individual i to infection by infected individual j (R_{ij}) which affects the probability individual i remains uninfected P_{ij}^S in each timestep, 2. The realized tumor growth rate r_i^{growth} for infected individual i , and 3. The “critical tumor load for survival” (see below) of infected individual i ($L_{S,i}^{crit}$), which affects weekly survival probability P_i^{surv} . Coevolution follows the phenotypic difference model such that each realized trait k is a function of the difference between the latent quantitative devil trait ($z_{k,i}$) and latent quantitative tumor trait ($x_{k,i}$ or $x_{k,j}$ depending on whether the trait is affected by an infected devil’s own tumor i or the tumor of another devil j). z_k is inherited according to the infinitesimal model of quantitative genetics while x_k evolves through mutation. We refer to z_k and x_k for a given k as a “trait-pair” and the coevolution of these trait-pairs serves as the focal point of our analysis. Our definitions of resistance and tolerance follow those of Råberg et al. (2009), where resistance is measured by a host’s ability to limit pathogen burden (in this case by reducing within-host tumor growth or resisting infection altogether) and tolerance measured by a host genotype’s fitness as a function of pathogen burden. The full overview, design concepts, and details (ODD) protocol (Grimm et al. 2006, 2010, 2020) may be found in Supplement 1. Figure 1 provides a graphical overview of the model structure and table 1 provides a list of variables, parameters, and notation.

Fig. 1. A visual schematic of the individual-based model. A) The simplified Tasmanian devil life-cycle used in the model. B) Devil inheritance, following the infinitesimal model of quantitative genetics. Colors represent the breeding values of the sire, dam, and offspring. C) DFTD epidemiology in a susceptible-exposed-infected (SEI) framework. Transmission and mortality are both functions of tumor volume, which increases stochastically and logistically over time. Bands in the tumor growth plot represent the 95% confidence interval for tumor volume at each point in time after infection.

Devil demographics

Devils are synchronous, annual breeders with a mating season typically lasting from late February to early April in the absence of DFTD (Jones et al. 2008; Pemberton 1990; Hesterman 2008; Hesterman et al. 2008). Most births occur from March to April and DFTD is not transmitted vertically (Pyecroft et al. 2007). As devils are altricial marsupials, young stay in the pouch for 4 months and the den for 6 months, usually dispersing from their natal site between December and April (Pemberton 1990; Rose et al. 2017). Devils typically become reproductively mature at age 2, although DFTD has led to an increase in precocial female breeding at age 1 in some sites (~14 months Jones et al. 2008; Lachish et al. 2009).

We model a simplified life history where mating occurs within a single week-long timestep, with each adult female reproducing with probability p_{mate} and multiple paternity (Russell et al. 2019). Female devils have four teats, limiting litter size to $b_{max} = 4$

offspring. Offspring survive to become independent with probability b_{prob} . Devils reproductively mature adults at age $a_{mat} = 2$ years, with no precocial breeding, last reproduce at age $a_{LR} = 5$ years, and die of old age at $a_{max} = 7$ years (Rose et al. 2017). Uninfected adults die at a rate d_A^{tot} , which is made up of a density-independent component d_{DI} and a density-dependent component $d_{DD}N$, where N is the number of devils. Subadult devils experience higher mortality rates than adults (Rose et al. 2017) such that per-capita juvenile death rate $d_{SA}^{tot} = d_{DI} + d_{SA} + d_{DD}N$ where d_{SA} is the excess subadult mortality.

Infection

DFTD is transmitted through biting during mating and competitive interactions (Hamede et al. 2013; Hamilton et al. 2019; Hamede et al. 2008; Hamilton et al. 2020). Because the effects of DFTD on devil behavior are not this study's focus, we assume simplified interactions with no spatial or social structure and frequency-dependent contacts (as this mode of transmission is most consistent with high DFTD prevalence in spite of strong population declines; McCallum et al. 2009): A devil interacts with other devils at a constant weekly rate $r_{contact}$ and encounters infected individuals at a rate $r_{contact} \frac{N_I}{N}$.

Let $P_{ij}^I(t)$ be the probability of successful infection given a contact between susceptible individual i and infected individual j at time t . If infection probability, population size, and number of infected individuals are approximately constant over a week, the number of successful transmissions is Poisson-distributed, and the probability that susceptible individual i remains susceptible at the start of the next week is

$$P_i^S = \exp \left[-\frac{N_I}{N} r_{contact} \bar{P}_i^I \right],$$

where $\bar{P}_i^I = \frac{1}{N_I} \sum_{j=1}^{N_I} P_{ij}^I$ is the average transmission probability given an infectious contact. We assume that co-infections by multiple tumors have no meaningful impact on disease progression. If multiple transmissions occur in the same week, the "first" infecting individual is randomly selected with probability $\frac{P_{ij}^I}{\sum_{j=1}^{N_I} P_{ij}^I}$.

We model P_{ij}^I as a logistic function of the log tumor load $\ln[L_j]$ of individual j . The maximum infection probability P_{max}^I is modified by the resistance of individual i to infection by individual j (R_{ij} , not to be confused with the basic reproduction number R_0) which is a function of the resistance genotype $z_{1,i}$ of devil i and the transmissibility genotype $x_{1,j}$ of tumor j . We then have

$$P_{ij}^I = P_{max}^I R_{ij} \frac{\left(\frac{L_j}{L_i^{crit}} \right)^\gamma}{1 + \left(\frac{L_j}{L_i^{crit}} \right)^\gamma} \quad (1)$$

where L_i^{crit} is the critical tumor load at which $P_{ij}^I = 0.5 P_{max}^I R_{ij}$ and γ is the logistic rate parameter. Thus,

$$P_i^S = \exp \left[-\frac{N_I}{N} \beta \bar{P}_i^I \right], \quad (2)$$

where $\bar{P}_i^I = \frac{\bar{P}_i^I}{P_{max}^I}$ and P_{max}^I has been combined with $r_{contact}$ to give the maximum transmission coefficient $\beta = P_{max}^I r_{contact}$. Because observed infections are much lower for subadults (Lazenby et al. 2018) due to higher pre-puberty anti-cancer immune capacity (Cheng et al. 2017) and lack of involvement in mating interactions, we assume that the subadult infection probability is reduced, relative to the adult infection probability, by fixed subadult resistance factor R_{SA} .

Tumor growth

We model tumor growth as stochastic, following Wells et al. (2017). Tumors have a latent period (τ) between the time of infection T_i^I and the time at which they become transmissible (McCallum et al. 2009; Espejo et al. 2022). The regression of visible tumors is very rare in natural populations (Margres et al. 2020), and the expected volume $\bar{L}_i(t)$ for tumor i , measured in cm^3 , increases logarithmically over time at genotype-dependent rate r_i^{growth} to maximum expected tumor size L_{max} (Hamede et al. 2017; Wells et al. 2017):

$$\bar{L}_i(t) = \frac{L_{max}}{1 + (L_{max} - 1)e^{-r_i^{growth}(t - T_i^I - \tau)}} - 1, \quad (3)$$

when $t \geq T_i^I + \tau$ and $L(t) = 0$ when $t < T_i^I + \tau$. We used a modified logistic growth function, with initial tumor load $L_0 = 0$, because the actual initial tumor load is small and difficult to estimate empirically. Equation 3 is approximately equal to the standard logistic curve for $L_{max} \gg 1$. We assume individual variation around $\bar{L}_i(t)$ is Gamma distributed with shape parameter $\lambda \bar{L}_i(t)$ and rate parameter λ (from Wells et al. 2017).

Mortality

Field studies demonstrate that tumor load affects body condition (Ruiz-Aravena et al. 2018) and mortality rate (Wells et al. 2017). We assume for simplicity that survival probability does not differ between males and females, so that if S_∞ is the fractional reduction in survival probability caused by a very large disease load, $L_{S,i}^{crit}$ is the critical disease load at which the reduction in survival probability is halfway between 1 and S_∞ , and α is the pathogenicity of the disease, we then have

$$P_i^{surv} = \left(\frac{1 + S_\infty \left(\frac{L}{L_{S,i}^{crit}} \right)^\alpha}{1 + \left(\frac{L}{L_{S,i}^{crit}} \right)^\alpha} \right) e^{-(d_{DI} + d_{DD}N)}. \quad (4)$$

Disease-related phenotypes and genetics

GWAS results show that a substantial proportion of variation in force of infection (FOI; calculated using time from age 1 to infection as an inverse proxy; Gallinson et al. 2024) and female devil survival after infection can be explained by a small number of large effect loci in devils (~20% and 76.5% of variation explained by an average of 2 and 4.8 SNPs, respectively Gallinson et al. 2024; Margres et al. 2018). However, FOI was more polygenic in tumors and female infection status was more polygenic in devils (16% and 38.3% of variation explained by an average of ~35 and 56.1 SNPs Gallinson et al. 2024; Margres et al. 2018). To avoid the potential complications of modeling coevolution in traits with differing genetic bases (e.g. Yamamichi and Ellner 2016), we chose to model coevolution in a purely quantitative genetic framework.

We assume that devils and tumors exhibit genetic variation in three disease-related phenotypes: Resistance to infection R_{ij} , tumor growth r_i^{growth} , and critical disease load for survival $L_{S,i}^{crit}$. Following the phenotypic difference model of coevolution (Nuismer 2017; Buckingham and Ashby 2022), we model the disease-related phenotypes as functions of the difference between latent devil traits z_1 , z_2 , and z_3 and latent tumor traits x_1 , x_2 , and x_3 , respectively. Resistance to infection R_{ij} is a logistic function of $z_{1,i} - x_{1,j}$,

$$R_{ij} = \frac{1}{1 + \exp[\omega_1(z_{1,i} - x_{1,j})]}. \quad (5)$$

where ω_1 is the intensity of the coevolutionary interaction. Both the mean initial devil phenotype, $\bar{z}_1(t=0)$, and the initial tumor phenotypes are zero so that the probability of infection for the average individual in a population first exposed to the disease is $\frac{1}{2}P_{max}^I$.

The tumor growth rate r_i^{growth} on an infected individual is

$$r_i^{growth} = \max\{r_0^{growth} - \omega_2(z_{2,i} - x_{2,i}), 0\}, \quad (6)$$

where r_i^{growth} is the initial tumor growth rate in a naive population and ω_2 is the intensity of the coevolutionary interaction. Because tumor regression is rare (0.01% of observed infections Margres et al. 2020), we assume that $r_i^{growth} \geq 0$.

The critical tumor size $L_{S,i}^{crit}$ of an infected devil deviates from the critical size in a DFTD-naive population $L_{S_0}^{crit}$ following the equation

$$L_{S,i}^{crit} = L_{S_0}^{crit}(1 + \omega_3(z_{3,i} - x_{3,i})), \quad (7)$$

where ω_3 is the intensity of the coevolutionary interaction. In practice, ω_1 , ω_2 , and ω_3 are not unique parameters, as changing the value of ω for any trait is equivalent to rescaling the variances of z and x for that trait (Supplement 1.7). We therefore set $\omega_1 = \omega_2 = \omega_3 = 1$.

The latent phenotype vector $\mathbf{z}_i = \{z_{1,i}, z_{2,i}, z_{3,i}\}$ for devil offspring i equals the vector of breeding values \mathbf{g}_i and the environmental deviation vector \mathbf{e}_i :

$$\mathbf{z}_i = \mathbf{g}_i + \mathbf{e}_i. \quad (8)$$

We assume the infinitesimal model (Fisher; Barton et al. 2017; Fisher 1918) such that \mathbf{g}_i is the average of the maternal (\mathbf{g}^f) and paternal (\mathbf{g}^m) breeding values plus a deviation due to recombination \mathbf{s}_i :

$$\mathbf{g}_i = \frac{1}{2}(\mathbf{g}_i^f + \mathbf{g}_i^m) + \mathbf{s}_i. \quad (9)$$

\mathbf{s}_i and \mathbf{e}_i are normally distributed with mean zero and covariance matrices \mathbf{S} and \mathbf{E} . In the absence of DFTD, and therefore selection, the devil genetic covariance matrix \mathbf{G} will converge to the initial devil genetic covariance matrix $\mathbf{G}(0) = 2\mathbf{S}$ (Walsh and Lynch 2018).

If the environmental component of a tumor's phenotype is normally distributed and constant during any given infection, then it may be merged with \mathbf{e}_i without loss of generality (Supplement 1.7). Tumor phenotype and genotype are therefore interchangeable. The latent genotype of a tumor on a newly infected devil is inherited asexually from the tumor on the infecting devil. Mutation and other within-tumor processes (Leathlobhair and Lenski 2022) cause a tumor's genotype to change slightly by an amount \mathbf{m} each week, such that $\mathbf{x}_i(t+1) = \mathbf{x}_i(t) + \mathbf{m}$. We assume non-directional mutation where \mathbf{m} is multivariate normal with mean zero and covariance matrix \mathbf{M} .

Parameter Selection

We parameterize the model with over 20 years of published results on devil demography, density, and genetics (e.g., Lazenby et al. 2018; Cunningham et al. 2021; Margres et al. 2018) by using sampled parameter sets to calculate demographic, epidemiological, and genetic quantities for which there were empirical estimates, and retaining parameter sets that yielded values consistent with those empirical estimates. This process followed a four-step procedure described in Supplement 2. Table 1 provide a list of model parameters and their notation and table 2 provides a list of studies upon which the parameter criteria are based. Of the 1,000,000 sampled parameter combinations, only 320 met all the criteria for inclusion in the final set, which we refer to as the "selected parameter values". Histograms of selected parameter values are given in Fig S1-S4 and the full list of selected parameters may be found in the supplementary data.

First, we Latin hypercube sampled 1,000,000 parameter sets from the initial range of parameters (Tables S2 and S3; see Supplement 2 for rationale). Second, for each set of parameters, we constructed an age-structured matrix population model describing pre-disease devil demographics. We then solved for the stable age distribution of the population and retained only parameter sets in which individuals age 2+ comprised 50 – 75% of the population, individuals age 3+ comprised 20 – 60% of the

population, and individuals age 4+ comprised 5 – 20% of the population, as empirically demonstrated in 12 sampling localities with multi-year mark-recapture data (Lachish et al. 2009; Hamede et al. 2012; Lazenby et al. 2018; see Supplement 2). We then chose death rates d_{DI} and d_{DD} such that the equilibrium population size was 200 individuals, corresponding to an area of roughly 150 km² (Lazenby et al. 2018; Cunningham et al. 2021). Due to stochasticity, stationary population sizes ranged in the individual-based model ~170-400, consistent with empirically-observed pre-DFTD densities (Cunningham et al. 2021).

Third, we calculated the survival probabilities and lifetime reproductive success (LRS) for an infected devil and basic reproduction number (R_0) for DFTD. We retained parameter sets with R_0 between 1 and 3 (McCallum et al. 2009) and LRS below replacement (Cunningham et al. 2021). Using mortality estimates from Wells et al. (Wells et al. 2017, Fig S2), we retained parameters for which 3 months survival after infection was >90%, 9 month survival was 25 – 75%, and 2 year survival was <20%.

Fourth, for each remaining parameter combination we ran 100 simulations for 20 years following the arrival of DFTD. We selected parameter combinations to ensure DFTD spread (mean DFTD prevalence in years 5 – 15 is >10%), devil decline (mean devil abundance in years 5 – 15 is <80% of initial abundance Cunningham et al. 2021), and devil-tumor coexistence (>80% probability) within the 20 year timeframe, since the longest infected populations have survived for at least this long. We then averaged the median and quartiles of the time from age 1 to infection (the force of infection proxy used by Gallinson et al. 2024), across simulations and retained only parameters in which the average 1st quartile was 10.8 – 51.9 weeks after age 1, the average median was 30.1 – 61.8 weeks, and the average 3rd quartile was 37.0 – 94.6 weeks (Gallinson et al. 2024; see Supplement 2). For each simulation, we calculated proportion of variance (PVE) in FOI, survival after infection, and case-control explained by devil or tumor genotype using the R^2 values of general linear models (Supplement 2). We retained parameters for which the average PVE in FOI by devil genotype was 2.7-20.0%, the average PVE by tumor genotype was 7.4-10.0%, and the average PVE by their interaction was 7.5-51.4% (Fig 2A in Gallinson et al. 2024). We also retained parameters for which the PVE in time to death by devil genotype was <27.6% and the PVE in case-control by devil genotype was 8.8-50.2% (Margres et al. 2018). The average PVEs in FOI by tumor genotype and average PVEs in time to death by devil genotype were far below the lower cutoffs, and we instead retained parameters above the 75th PVE percentile (across parameter combinations) for each of these quantities.

Model Implementation

The individual-based simulations and parameter selection process were implemented in R version 4.3.0 (R Core Team 2023) and C++ 20 (Stroustrup 2013) using the Rcpp package (version 1.0.10; Eddelbuettel et al. 2023). Each post-DFTD simulation was initialized by sampling the starting devil abundance and age-structure from a 1000 year time-series of a simulated DFTD-free population (with a 100 year burn-in period). Initial devil genotypes were multivariate normal with mean zero and initial devil genetic covariance matrix $\mathbf{G}(0)$. Ten randomly-selected adults were initially infected to ensure DFTD spread. Tumor genotypes were all initialized to $\mathbf{x}_i = 0$, corresponding to “baseline” tumor transmissibility, growth rate, and virulence. Each simulation was run for 100 years (i.e., 50 devil generations and 5200 weekly time steps).

Results

The effect of genetic variation on realized trait variation

We used initial devil genetic variance and tumor mutation variance (diagonal entries of $\mathbf{G}(0)$ and \mathbf{M}) as proxies for the evolvability of latent devil and DFTD traits. Figure 2 relates devil and tumor genetic variation to variation in the realized disease-related traits. To isolate the effects of devil variation from tumor variation, and vice versa, we make the following simplifications: In the first column of Figure 2, we plot the variation in the realized traits as a function of devil genetic variation assuming that $t = 0$ (i.e., the arrival of DFTD). In the second column of Figure 2, we plot variation in the disease-related traits as a function of accumulated tumor mutation variance for a long-lived (2-year-old) tumors at the arrival of DFTD ($x_i = 0$) infecting devils with phenotype $z_i = 0$. These assumptions isolate the accumulated tumor mutation variance from both devil phenotypic variance and preexisting tumor genetic variance. Analytic equations for the curves in both columns are derived in Supplement 1. The third column of figure 2 shows variation in the disease-related traits from all sources over time. The 95% confidence bands for these panels were computed over 1000 simulated devil-tumor pairs and included variation in devil phenotype, tumor mutation, and stochastic tumor growth (see supplement 1). For these simulations, all parameters were set to their mean selected values.

Fig. 2. The relationship between initial devil genetic variance, tumor mutation variance, and variation in disease-related traits. The first column shows the variation (95% quantile bands) in disease-related traits due to devil genetic variance at the arrival of DFTD, when all tumors have the same genotype $x_{1,i} = 0$. These disease-related traits are A) the probability of infection given contact P_{ij}^I as a function of tumor size, D) tumor size (cm³) as a function of weeks since infection, and G) weekly survival probability as a function of tumor size. Colors denote different values of initial devil genetic variance. The second column shows the variation (95% quantile bands) in B) the probability of infection given contact, E) tumor size, and H) weekly survival probability due to genetic variation among 2-year-old tumors that, after initially having the same genotype $x_{1,i} = 0$, diverged due to mutation. Colors denote different values of DFTD mutation variance. Note that all curves in the first and second columns represent function-valued traits rather than realized values (e.g. 2-year-old tumors are unlikely to actually be less than 1 cm³). The third column shows the variation (95% quantile bands) in disease-related traits due to all sources of variation at the arrival of DFTD. These traits are C) the cumulative probability of infection for susceptible devils, F) tumor growth, and I) cumulative devil survival, all given as a function of weeks since infection. Note that panel C assumes that only the 10 initially infected devils are infectious (i.e., secondary infections are discounted) and therefore underestimates infection probability. The red boxes in column 3 indicate that the panels in this column are not directly comparable to those in columns 1 and 2. Unless otherwise specified, all parameters are set to their mean selected values.

From Figure 2 we may observe the following two patterns: First, initial devil phenotypic variation is substantial, with the mean selected parameters yielding a meaningful fraction of initial devils with low infection probability and with high survival probability (at least within a two year timeframe; Fig 2C,F,I). Note, however, that though figure 2C shows cumulative infection probability flattening over time, this is most likely an artifact of discounting secondary infections. In reality, once the secondary contacts themselves become infectious, there would be a rapid increase in infection probability due to higher DFTD prevalence. Second, tumor mutation generates a meaningful amount of trait variation during a single devil generation (Fig 2B,E,H). In addition to indicating rapid accumulation of tumor genetic variance, this result also illustrates that disease-related traits may change over the course of a single infection.

Theoretical coevolutionary dynamics

We first examined the range of dynamics theoretically possible for coevolution in single devil-DFTD traits pairs. We ran 1000 simulations for each point in a 20×20 grid (Fig 3) across the range of initial devil genetic variances and tumor mutation variances. For each trait-pair examined, the variances of the other two trait-pairs were set to zero (preventing evolution in those trait pairs) while each remaining parameter was set to the mean of its selected values (i.e those consistent with empirical data).

Fig. 3. Devil population outcomes for coevolution in single pairs of devil-DFTD traits. Top row: the probability of devil persistence to 50 devil generations (100 years) after the introduction of the devil facial tumor disease (DFTD), for coevolution in A) tumor transmissibility and devil resistance to infection, B) tumor growth and devil resistance to tumor growth, C) tumor virulence and devil tolerance, plotted as a function of the initial genetic variation in devil resistance to infection at the arrival of DFTD (x-axis) and weekly tumor mutation variance in tumor transmission (y-axis). Bottom row: the probability of devil-DFTD coexistence to 50 devil generations for coevolution in D) transmissibility / infection resistance, E) tumor growth, F) virulence / tolerance. Probabilities are calculated over 1000 simulated populations. Other parameters were set to their respective averages over all empirically consistent parameter values.

When tumor transmissibility and devil resistance to infection coevolve, devil persistence depends on relative evolvability of devil and tumor traits (Fig 3A,D and Fig S5A,D). Greater tumor mutation variance (faster tumor evolution) increased the likelihood of devil extirpation while greater initial devil genetic variance (faster devil evolution) increased the likelihood of tumor extirpation (Fig 3A,D). The evolutionary dynamics for fixed values of tumor mutation variance and devil genetic variance confirm simulations that ended in devil extirpation had faster DFTD evolution on average than simulations that ended in devil persistence and DFTD extirpation (Fig S6, S7). Greater tumor mutation variance in tumor virulence and greater initial genetic variance in devil tolerance decreased the likelihood of devil extirpation and increased the likelihood of devil-tumor coexistence (Fig 3C,F).

Devil ecological outcomes under coevolution of tumor growth rate and devil resistance to tumor growth differ from the outcomes under coevolution of resistance to infection in several key ways (Fig 3B,E and Fig S5B,E). First, greater tumor mutation variance had only a marginal effect on devil persistence for low values of initial devil genetic variance (<0.004). Thus, in a “tumor evolution only” scenario the relationship between tumor mutation variance and devil persistence is much flatter when tumor growth rate evolves than when tumor transmissibility evolves. Further, the minimum devil persistence probability across parameters is greater under evolution of tumor growth and devil resistance to tumor growth than under coevolution of resistance to infection and transmissibility (16.5% compared to 9.4%). Second, the maximum probability of devil-DFTD coexistence across parameters is also far greater under coevolution of tumor growth and devil resistance to tumor growth (40.5% compared to 4.1%; Fig 3E) and the mean times to devil and DFTD extirpation are longer than under coevolution of resistance to infection and transmissibility (Fig S5; note the different scale bars). Third, in the case of only devil evolution (Fig 3A,B near the x-axis), the rate of increase in devil persistence with devil genetic variance is relatively stable when resistance to infection evolves, while under evolution of resistance to tumor growth, persistence increases relatively slowly at low variance values before sharply increasing around 0.005.

Empirically-consistent coevolutionary dynamics

Second, we examined the coevolutionary dynamics of single devil-DFTD trait pairs across all selected parameter values, setting the variances of the two non-focal trait pairs zero but allowing a other selected parameters to vary (i.e., each point in Fig 4 represents a different combination of all parameters). Parameter values with low devil genetic variance and high tumor mutation variance were more likely to be excluded during parameter selection (Fig 4a; Fig S9). Exclusion is most pronounced for transmissibility/resistance to infection and tumor growth/resistance to tumor growth. Notably, while the selected parameter values skew heavily towards smaller values of tumor mutation variance and moderate to high values of devil genetic variance, they still encompass significant variation in devil persistence probability (Fig 4; more clearly illustrated in Fig S9).

Fig. 4. Empirically-consistent parameter values for initial devil genetic variance and tumor mutation variance for each devil-DFTD trait pair. A) Initial variance in devil resistance to infection at the arrival of DFTD (x-axis) and mutation variance in tumor transmissibility (y-axis). B) Variance in devil resistance to tumor growth and in tumor growth rate. C) Variance in devil tolerance to tumor load and in tumor virulence. White contour lines denote the density of the parameter values. Each point's color represents the probability of devil persistence, calculated over 1000 simulated populations, for that parameter combination assuming coevolution in only the focal trait pair.

Devil persistence probabilities under coevolution of both transmissibility/resistance to infection and coevolution of tumor growth/resistance to tumor growth are robust to uncertainty in other model parameters (compare Fig 3A to Fig 4A and Fig 3B to Fig 4B), but are sensitive to parameter uncertainty under coevolution of virulence/tolerance. When persistence probabilities under

virulence/tolerance coevolution were calculated over all selected parameter combinations rather than the mean parameter values (Fig S9A), the average probability of devil persistence was 33.1%, and more than half (52.1%) of parameter combinations resulted in devil persistence probabilities of <25%.

Third, we examined the population and evolutionary dynamics when all three trait-pairs coevolve simultaneously (Fig 5) and compared them to the dynamics when only one trait-pair was allowed to coevolve (Fig S6-S7). To illustrate the evolutionary dynamics of each trait-pair, we focus on the mean values of “net devil resistance” ($z_{1,i} - x_{1,i}$), tumor growth rate r_i^{growth} and “net devil tolerance” ($z_{3,i} - x_{3,i}$). These measures show the net effect on devil-DFTD coevolution in each trait-pair over time. In each instance, we ran 1000 simulations with each parameter equal to its mean selected parameter value and, for the single trait-pair runs, the variances of the other two trait-pairs set to zero.

Fig. 5. The dynamics of devil population size, devil facial tumor disease (DFTD) prevalence, and devil-DFTD coevolution for all three trait-pairs. A) Devil population size over 1000 simulated populations, grouped based on population outcome. B) DFTD prevalence. C) Average net devil resistance, defined as the resistance phenotype of a devil minus the transmissibility phenotype of the tumor infecting it, averaged over all infected devils in the population in each year. D) Tumor growth rate, also averaged over all infected devils in the population. E) Average net devil tolerance, defined as the tolerance phenotype of the devil minus the virulence phenotype of the tumor infecting it. Blue denotes simulations in which both devils and DFTD persisted to 50 devil generations after the arrival of DFTD, red denotes simulations in which the devil population was extirpated, and black denotes simulations in which DFTD was extirpated. Solid lines denote the median value over time for each group of simulations and bands denote the interquartile range. Parameters were set to their respective averages over all empirically-consistent parameter values.

When all three trait-pairs coevolved simultaneously under the mean selected parameters, DFTD evolved greater transmissibility and greater tumor growth rate faster than devils evolved resistance to infection or to tumor growth (Fig 5). Simultaneously, devils evolved greater tolerance and DFTD evolved reduced virulence, leading tumor prevalence to increase to an average of around 60% across simulations. There was a 74.7% probability of devil-tumor coexistence, which was strongly driven by the coevolution of reduced tumor virulence and increased devil tolerance. When only tumor transmissibility and devil resistance to infection coevolved, 78.8% of simulations resulted in devil extirpation, 21.2% showed DFTD extirpation and devil persistence, and no of simulations showed devil-DFTD coexistence (Fig S6). Simulations in which devils persisted showed faster evolution of devil resistance than evolution of DFTD transmissibility, while simulations in which devils went extinct showed the opposite. When there was coevolution of tumor growth and devil resistance to tumor growth, 84.5% of simulations experienced devil extirpation (DFTD extirpation: 15.4%, devil-DFTD extirpation: 0.1%) and, for all simulations, tumor growth rate decreased from its initial value.

Does coevolution promote devil-DFTD coexistence relative to a non-evolving population?

Finally, to quantify the global sensitivity of devil persistence, devil-DFTD coexistence, and devil recovery to coevolution in each trait pair (Fig 6,7), we ran four sets of 1000 simulations, for each set of selected parameters, in which either all devil and DFTD traits were allowed to coevolve or one devil-DFTD trait-pair had its variances set to zero while the other two were allowed to coevolve (i.e., “leave one out”). We further ran a set of 1000 simulations in which evolution in both devils and DFTD was entirely absent, which served as the point of comparison by which to assess the effect of coevolution. This analysis also quantified the global sensitivity of devil persistence and devil-DFTD coexistence to the total uncertainty across all model parameters (Tables S4,S5).

Fig. 6. The distribution of probabilities of devil persistence and devil – devil facial tumor disease (DFTD) coexistence. A) The probability of devil persistence and B) the probability of devil-DFTD coexistence across parameter combinations when, in order from left to right, 1. There was no evolution (this plot is not included in panel B, as the probability of devil-DFTD coexistence was zero for nearly all parameter combinations), 2. Tumor transmissibility and devil resistance to infection are prevented from coevolving, but all other trait-pairs are allowed to coevolve, 3. Tumor growth rate and devil resistance to tumor growth are prevented from coevolving, 4. Tumor virulence and devil tolerance are preventing from coevolving, and 5. All three trait-pairs coevolve simultaneously. The lines in each violin plot represent, in ascending order, the 25th percentile, the median, and the 75th percentile of probabilities in the distribution. The probabilities of devil persistence and tumor extirpation were calculated over 1000 simulated populations for each parameter combination and are shown within each distribution as a beeswarm plot of points.

Fig. 7. The average devil population recovery in the event of devil - devil facial tumor disease (DFTD) coexistence. The ratio between the final devil population size, 50 devil generations (100 years) after the arrival of DFTD, and the initial devil population size, averaged over simulations in which there was devil-DFTD coexistence. The violin plots represent, in order from left to right, scenarios where, 1. Tumor transmissibility and devil resistance to infection are prevented from coevolving, but all other trait-pairs are allowed to coevolve, 2. Tumor growth rate and devil resistance to tumor growth are prevented from coevolving, 3. Tumor virulence and devil tolerance are preventing from coevolving, and 4. All three trait-pairs coevolve simultaneously. The lines in each violin plot represent, in ascending order, the 25th percentile, the median, and the 75th percentile of recovery proportions across empirically-consistent parameter values. Proportional devil recoveries were calculated over 1000 simulated populations for each parameter combination and are shown within each distribution as a beeswarm plot of points. Parameter combinations in which no simulations resulted in coexistence are excluded.

We observed a high probability of devil persistence to 50 generations (100 years) after disease introduction (median 77.0%; Fig 6A), which was robust to parameter uncertainty (interquartile range 58.3-91.7%); only 16.5% of parameter combinations resulted in devil persistence probabilities of <50%. We also observed a high probability of devil-DFTD coexistence. In simulations

when devils persisted, DFTD had a median 74.4% chance of also persisting, corresponding to a median coexistence probability of 50.2% over all simulations (Fig 6B). However, the coexistence probability was sensitive to parameter uncertainty: the probability of DFTD persistence given devil persistence had an interquartile range of 46.5-89.8% and the overall coexistence probability had an interquartile range of 27.2-74.4%. The median average time to devil extirpation was 36.1 years (interquartile range of 30.5-41.8 years), and the median average time to tumor extirpation was 33.8 years (interquartile range of 27.6-41.8 years). Tables S4 and S5 give the Spearman partial correlation coefficients between each parameter, devil persistence and devil-DFTD coexistence. For simulations in which devils and DFTD coexisted for 50 generations, devils recovered to a median, across parameters, average of 62.0% their original population size (interquartile range: 44.7-75.9%; Fig 7). Only 34.6% of parameter combinations had an average recovery of less than 50% for simulations with devil-DFTD coexistence (Fig 7). Parameters with the highest probability of devil-DFTD coexistence also had the highest percent recovery among simulations in which coexistence occurred (Spearman correlation = 0.588; Fig S10). By contrast, in the absence of evolution, devil persistence was low (median 14.5%; interquartile range: 9.9%-21.5%; Fig S9) and devil-DFTD coexistence was almost nonexistent (median: 0%; interquartile range: 0%).

Sequentially preventing the coevolution of a single trait-pair while allowing the other two to coevolve (i.e., “leave one out”) led to similar reductions in devil persistence probability when coevolution in transmissibility / resistance to infection and in tumor growth / resistance to tumor growth were omitted (with median persistence probabilities of 53.4% and 47.5%, respectively; Fig 6A) and a smaller reduction when coevolution of virulence/tolerance was omitted (61.6%; Fig 6A). Removing the coevolution of devil tolerance and tumor virulence dramatically decreased the probability of coexistence (median value 1.7%) while removing coevolution in tumor growth rate and in transmissibility/resistance to infection led to a smaller decreases (medians 30.0% and 41.75%, respectively; Fig 6B). The omission of coevolution in devil tolerance and tumor virulence also reduced the median average devil population recovery among simulations with coexistence (42.4% of initial population size; 62.8% and 61.7% with the removal of coevolution in transmissibility/resistance to infection and coevolution in tumor growth rate, respectively; Fig 7).

Discussion

DFTD has caused declines of up to 80% in most infected Tasmanian devil populations (Lazenby et al. 2018; Storfer et al. 2018; Cunningham et al. 2021) and initial ecological models predicted devil extinction (McCallum et al. 2009; Beeton and McCallum 2011). Nonetheless, long-diseased devil populations (>20 years) have persisted at low densities (Lazenby et al. 2018; Cunningham et al. 2021). Substantial evidence of evolution has been found in both devils and DFTD (Epstein et al. 2016; McLennan et al. 2018; Patton et al. 2020; Stammnitz et al. 2023; Stahlke et al. 2021), suggesting that coevolution may, in part, be driving continued devil persistence. To test the effect of coevolution on devil persistence, we developed one of the first models that integrates multivariate genetic coevolution with individual-based host-pathogen dynamics to predict host extinction risk. We found that empirically-consistent values of genetic variance for devil traits associated with DFTD resistance and tolerance were sufficient to allow rapid devil evolution and that devil-DFTD coevolution had consistently positive effects on devil persistence relative to a non-evolving population. Multivariate coevolution led to higher probabilities, relative to previous model scenarios without evolution, of devil persistence (78.1%) and devil-DFTD coexistence (56.5%) for at least 50 devil generations (100 years), with the latter driven primarily by the evolution of greater devil tolerance and reduced DFTD virulence. Moreover, while ecological models predict that devil-DFTD coexistence limits devil populations to, on average, 9% (Siska et al. 2018) and 48% (Wells et al. 2019) of their pre-disease abundance, we found that coevolution of devil tolerance and DFTD virulence enabled devil populations to slowly recover, despite DFTD, to an average of 60.6% of their initial abundances after 100 years, and that the degree of devil recovery was strongly correlated with the likelihood of devil-DFTD coexistence. Given that devils act ecologically as both the apex predator and scavenger in Tasmania (Cunningham et al. 2018; Cunningham et al. 2020), these differences in predicted population size could have substantial effects on the mammalian community. Taken together, these results suggest rapid devil-DFTD coevolution may have strongly contributed to continued devil persistence and will likely play an important role in shaping long-term devil-DFTD dynamics.

Coevolutionary dynamics

We modeled the coevolution of three pairs of disease-related traits: 1) tumor transmissibility and devil resistance to infection (measured by the probability of infection given contact); 2) tumor growth and devil resistance to tumor growth (measured by a tumor's logistic growth rate); 3) tumor virulence and devil tolerance (measured by the disease-related morality rate). We found very few empirical constraints on which phenotypic traits may be rapidly evolving (Fig 4), suggesting that evolution is multivariate and its effect on devil persistence is driven by the interaction between coevolving trait-pairs (Fig 6; Tables S4,S5). Consistent with the phenotypic difference model of coevolution (Nuismer 2017), both the coevolution of tumor transmissibility and devil resistance to infection, and the coevolution of tumor growth rate and devil resistance to tumor growth, exhibited arms race dynamics that most often led to either devil (47.8% and 33.4%) or tumor extirpation (48.8% and 37.5% of simulations, respectively, at the mean parameter values; Fig S6,S7). Meanwhile, the evolution of lower tumor virulence and increased devil tolerance increased both tumor prevalence and the probability of devil-DFTD coexistence (84.7%; Fig 5), consistent with theoretical predictions for the effect of virulence and tolerance evolution on disease persistence (Roy and Kirchner 2000; reviewed in Searle and Christie 2021).

Parameter combinations with high tumor mutation variance and low initial devil genetic variance were the most likely to generate predictions inconsistent with empirical data (Fig 4), indicating that evolutionary changes in tumor transmission and growth are unlikely to be driven by DFTD evolution alone and that devil-DFTD coevolution is likely occurring across multiple traits. Despite reduced devil genetic diversity due to historical bottlenecks (Miller et al. 2011; Brüniche-Olsen et al. 2014; Brüniche-Olsen et al. 2016; Brüniche-Olsen et al. 2018; Gooley et al. 2020), our results are consistent with genome-wide scans for selection and GWAS results suggesting that devils retain sufficient standing genetic variation to respond rapidly to the strong selection imposed by

DFTD (Epstein et al. 2016; Margres et al. 2018; Fraik et al. 2020; Stahlke et al. 2021). Indeed, allele frequencies in SNPs associated with genes conferring antigen presentation and cell communication increase significantly in as few as 4-6 generations following the arrival of DFTD (Epstein et al. 2016; Fraik et al. 2020; Stahlke et al. 2021). Though variation in mutation rates between DFTD lineages (Stammnitz et al. 2023) is likely an important component of DFTD evolution, we could not use these estimates to inform our mutation variance parameters, which are expressed in phenotypic units. The empirical constraints imposed on tumor mutation variance did not constrain the range of demographic outcomes under univariate coevolution. When tumor transmissibility coevolved with devil resistance to infection, for example, the probability of devil persistence ranged from >80% to <20% (Fig 4). Thus coevolution in any one trait-pair was not sufficient to ensure devil persistence.

When either DFTD transmissibility and devil resistance to infection coevolved alone or tumor growth and devil resistance to tumor growth coevolved alone, devil traits tended to evolve faster than DFTD traits in scenarios where devils persisted, resulting in decreased probabilities of infection and slower tumor growth (Figs S3,S4). In contrast, when all three trait-pairs coevolved, tumor growth rate and the probability of infection both increased significantly despite evolution of increased devil resistance. It is unlikely that these increases were driven by negative correlations between devil resistance and tolerance. We did not impose any *a priori* assumptions on the correlation between devil traits and the only correlation with moderate support from empirical data was a positive correlation between devil resistance to tumor growth and devil tolerance (66.9% of selected parameters; Fig S4). There was also evidence for negative correlation between DFTD virulence and transmissibility (70.9% of selected parameters; Fig S4), which could explain the increase in DFTD transmissibility but not the increase in growth rate (which was positively correlated with virulence for 61.7% of selected parameters). Rather, the decrease in DFTD-related devil mortality due to reduced tumor virulence and greater devil tolerance likely decreased the negative fitness consequences of DFTD for infected individuals. This result is consistent with previous models of host evolution (Restif and Koella 2004; Singh and Best 2021) that predict lower pathogen virulence reduces selective pressure for host resistance while increasing selective pressure for host tolerance. The evolution of reduced DFTD virulence and increased devil tolerance may therefore play a critical role in driving devil-DFTD dynamics. Indeed, female tolerance of DFTD, relative to males, has already been demonstrated, with female body condition declining by less than 5% when tumour weight reaches approximately 6% of host body mass (Ruiz-Aravena et al. 2018).

Coevolution promotes coexistence between devils and DFTD

In contrast to previous compartmental and individual-based ecological models (McCallum et al. 2011; Wells et al. 2019), we found that coevolution leads to a high probability (median: 58.9%) of devil-tumor coexistence for at least 50 generations (100 years). Devil persistence was driven by a combination of evolution in all three disease-related traits, while DFTD persistence was driven primarily by the evolution of tolerance in devils and reduced DFTD virulence (Fig 6). Though predictions of devil persistence were robust, the predicted probability of devil-DFTD coexistence was sensitive to parameter uncertainty.

Wells et al. (2019), whose model did not include evolution, reported a probability of devil extirpation similar to our results (21% to our average 27.1% across parameters when all three trait-pairs coevolve) but with higher probability of tumor extirpation (57% to our 23%) and lower probability of devil-tumor coexistence (22% to our 49.6%). This difference is likely driven by the evolution of devil tolerance and reduced DFTD virulence, as the tumor extirpation probability rises to a mean of 54.6% when the evolution of tolerance is omitted.

By contrast, the ecological model developed by Siska et al. (2018) predicted devil-DFTD coexistence at the metapopulation level for all 200 most realistic parameter combinations. They attribute this high coexistence probability to the ability of devils and DFTD to recolonize patches in the event of local extirpation, a feature not included in our model. Given typically large devil dispersal distances (i.e., genetic spatial autocorrelations suggesting 30 km on average, but up to 109 km; Lachish et al. 2011; Storer et al. 2017) and high population connectedness (i.e., devils form only three genetic clusters across the entirety of their geographic range; Hendricks et al. 2017), possible metapopulation dynamics likely play an important role in the island-wide persistence of devils and, if included in our model, may result in a similarly high probability of devil-DFTD coexistence.

Notably, while Wells et al. (2019) and Siska et al. (2018) predict that devil-DFTD coexistence prevents devil populations from returning to their pre-disease abundance (with devils at an average of 48% and median of 9% of their pre-disease abundance, respectively) and results in population cycles (Wells et al. 2019), we find that the evolution of reduced tumor virulence and greater devil tolerance can enable devil populations to slowly recover, in spite of DFTD (we did not quantify population cycling within this broader trend). Though we found an average population recovery to 60.6% of starting abundance, recovery was strongly correlated with the probability of devil-DFTD coexistence such that selected parameters with a high probability of devil-DFTD coexistence also show a high probability of devil recovery (Spearman $\rho = 58.8$; Fig S10).

Wells et al. (2019) also found more rapid devil and tumor extirpation, with times to devil extirpation concentrated between generations 5-10 (10-20 years), with a long tail, and times to tumor extirpation concentrated between generations 5-15 (our model predicted an interquartile range of 15-21 generations for mean time to devil extirpation and 14-21 generations for mean time to tumor extirpation). This difference likely occurred in part because we selected parameters to ensure neither devil nor DFTD extirpation occurred within the first 10 devil generations, consistent with lack of any observed extirpation among continuously distributed wild populations (Cunningham et al. 2021).

Though we chose to model devil-DFTD coevolution in a quantitative genetic framework, selection at large-effect loci may play an important role in rapid devil-DFTD coevolution. Margres et al. (2018) found that ~ 7 loci explain 60.6% of genetic variation in devil tolerance. Evolution is predicted to proceed more rapidly in traits determined by a mix of large-effect and small-effect loci than in traits determined by small-effect loci alone, with a transient increase in genetic variance driven by the large-effect loci (Gomulkiewicz et al. 2010). It is therefore possible that parameterizing a purely quantitative genetic model with results of Margres et al. (2018) inflated our empirically-plausible values of tolerance variance. However, our qualitative results are robust even if the maximum initial devil genetic variance in tolerance is halved (Figures S11) and, while devil-DFTD coexistence correlates with devil

tolerance, coexistence is more sensitive to DFTD mutation variances and correlations (Table S5). In 2014, a second DFT strain of independent origin (DFT2) was discovered in the southeast of Tasmania. This strain originated from a male devil, as opposed to a female in the case of DFTD (James et al. 2019), has an elevated mutation rate relative to DFT1, and has already diverged into two distinct lineages (Stammnitz et al. 2023). We did not consider DFT2 in the present study, as it is believed not to have spread beyond its region of origin (James et al. 2019). However, within-host competition between disease strains can counterbalance between-host selection for reduced virulence (reviewed in Alizon et al. 2013). Therefore, if DFT2 were to spread more widely, our prediction of reduced DFTD virulence may not hold and the likelihood of devil-DFTD coexistence could be significantly affected.

Broader Implications and future directions

Implications for Coevolutionary Theory

Our multivariate model of host-disease coevolution represents an important contribution to the theory of disease ecology and coevolution. Previous modeling studies have examined simultaneous evolution of host resistance and tolerance (Restif and Koella 2004; Råberg et al. 2007; Boots et al. 2009; Boots and Best 2018), evolution of pathogen virulence and transmission (Alizon et al. 2009; Cressler et al. 2016), and, separately, the coevolution of pathogen transmission and host resistance (reviewed in Buckingham and Ashby 2022) and the coevolution of within-host pathogen growth and host immune response (Gilchrist and Sasaki 2002). However, host-disease models that are both multivariate and coevolutionary remain rare (but see multi-step infection models such as Fenton et al. 2012; Nuismer and Dybdahl 2016, and gene/protein network models such as Kamiya et al. 2016; Shin and MacCarthy 2016) and, to our knowledge, our model represents one of the first to examine the effect of multivariate coevolution on host and pathogen extirpation risk. Considering coevolution in a multivariate context is important because the transmission and within-host growth of a disease are multi-step processes that depend on behavioral patterns of contact, host immune responses, and the biology of the disease (reviewed in McCallum et al. 2017; Handel and Rohani 2015; Hall et al. 2017). Selection may act on host or pathogen traits at each of these multiple steps and, as our results highlight, the traits on which selection acts may dramatically affect the host population outcome of an epizootic disease outbreak.

DFTD's slow growth and load-dependent effect on host fitness are features shared by other high-profile wildlife diseases, including chytridiomycosis in amphibians (Voyles et al. 2009; Grogan et al. 2023; Voyles et al. 2018) and white-nose syndrome in North American bats (Blehert et al. 2009; Hoyt et al. 2021). The shape of the load-dependent infection and mortality curves has been shown to critically influence host population persistence of both frogs and bats (Wilber et al. 2017; Langwig et al. 2017). Though there are important differences between these diseases and DFTD (such as environmental transmission and temperature-dependent growth; Wilber et al. 2017; Hoyt et al. 2021), our results suggest that host and pathogen trait correlations are likely to play an important role in these systems as well. Indeed, Wilber et al. (2024) found that evolution in each of three different host traits, analogous to the devil traits we consider, had substantially different effects on the time to host-population recovery during a chytridiomycosis outbreak.

Phenotypic tradeoffs or genetic correlations between traits are critical constraints on evolution in both hosts and pathogens (for example, physiological or immunological costs of host resistance; Núñez-Farfán et al. 2007, resistance-tolerance tradeoffs in hosts; Restif and Koella 2004; Råberg et al. 2007; Boots et al. 2009; Boots and Best 2018; Singh and Best 2021, and transmission-virulence trade-offs in pathogens, reviewed in Cressler et al. 2016) and, indeed, genetic and mutational correlations were among the parameters to which our results were most sensitive (Table S5). In this context, it is surprising that we found evidence for a negative correlation between DFTD transmission and virulence. No study has yet examined the genetic correlation between disease-related traits in devils or DFTD and therefore the only empirical constraints on these correlation parameters in our model were likely imposed by the purely demographic selection criteria. The importance of these correlations to devil persistence emphasizes the need for continued research into the genomic basis of devil and DFTD traits and the broader need to consider rapid host-disease coevolution in a multivariate context.

Implications for devil conservation

Tasmanian devils are a charismatic species of global interest and are the focus extensive conservation and research efforts. Early post-discovery of DFTD, a captive "insurance" population was established across zoos and wildlife parks throughout Tasmania with the aim to either reintroduce devils in cases of extirpations or supplement declining populations to enhance their genetic diversity (CBS 2008). Later, devils were introduced onto Maria Island, which had no prior history of Tasmanian devil presence (DPI 2010; Hogg et al. 2017, 2015). The conservation efficacy of translocating devils from this disease-free insurance population to low-density infected populations has been the subject of ongoing discussion (Hohenlohe et al. 2019; Hamede et al. 2021), with limited translocations having occurred in four natural populations (Glasscock et al. 2021). Although translocation has the potential to benefit devil populations at low abundance by raising population size and potentially alleviating inbreeding depression (i.e. genetic rescue, reviewed in Whiteley et al. 2015; Hedrick and Garcia-Dorado 2016; Grueber et al. 2019), the introduction of DFTD-naïve individuals risks exacerbating the epidemic and causing outbreeding depression by disrupting the population's adaptation to DFTD (Hohenlohe et al. 2019; Hamede et al. 2021). Our predictions that coevolution promotes devil persistence and could even allow devils to regain a substantial fraction of their original abundance adds to growing evidence that translocation may not be necessary to prevent devil extinction (Wells et al. 2019; Cunningham et al. 2021). An important caveat to our result is that our model did not include inbreeding or any other Allee effect that could lead to extirpation if devil abundance drops below a minimum viable population size (Frankham et al. 2014; Luque et al. 2016). Evidence for DFTD-induced increases in devil inbreeding depression remains equivocal (Brüniche-Olsen et al. 2014; Gooley et al. 2020; Lachish et al. 2011) and the level of inbreeding depression necessary to threaten devil extinction is currently unclear. A critical next step therefore is to incorporate inbreeding into eco-evolutionary models to determine its effects on devil persistence.

Supplementary Material.

Supplementary material is available online at *Evolution*.

Data Availability.

The model scripts and output data files are available on Dryad at <https://doi.org/10.5061/dryad.crjdfn3c7>.

Author Contributions.

Conceptualization: DTC, AS, RKH, MEJ, MJM, HM. Data Curation: DTC. Formal Analysis: DTC. Methodology: All authors. Funding Acquisition: AS, RKH, MEJ, MJM, HM. Resources: DGG, RKH, MEJ, MJM. Software: DTC. Supervision: AS, MEJ, HM, MJM, RKH. Validation: All authors. Visualization: DTC. Writing – Original Draft: DTC, AS. Writing – Review and Editing: All authors.

Funding.

The study was funded by the National Science Foundation (<https://www.nsf.gov>) DEB 2027446 to M.J.M., A.S., M.E.J., and H.M. and DEB 2324456 to M.J.M., A.S., and R.K.H. R.K.H. was also supported by the Australian Research Council (<https://www.arc.gov.au>) ARC-DE170101116 and ADR-LP170101105, the Centre National de la Recherche Scientifique (<https://www.cnrs.fr/en>) International Associated Laboratory Grant, the Agence National de la Recherche (<https://anr.fr/en/>) ANR- TRANSCAN 18-CE35-0009, and the MAVA Foundation (<https://mava-foundation.org>). This research used resources of the Center for Institutional Research Computing at Washington State University. The funders did not play any role in the study design, model formulation and analysis, decision to publish, or preparation of the manuscript.

Conflict of interest. The authors declare no conflict of interest.

Acknowledgments. We thank Douglas Kerlin and David Hamilton for their feedback on the formulation of the model.

Alt text for figure 1: Panel A shows a timeline of devil life events from birth to death. Panel B shows a ball-and-stick diagram of the infinitesimal model of quantitative genetics. Panel C shows a box and stick diagram of the susceptible-exposed-infected (S E I) model with sub-figures showing infection probability, tumor growth, and devil mortality as functions of tumor size, time, and tumor size, respectively.

Alt text for figure 2: Plots of individual-level variation in disease related traits, with subfigures labelled from A to I, due to variation from devils, tumors, and all sources.

Alt text for figure 3: Colored contour plots of devil persistence probability, and devil and devil facial tumor disease coexistence probability.

Alt text for figure 4: Lined contour plots showing the density of selected values of tumor mutation variance and devil genetic variance for each of the three trait-pairs (panels A through C). The raw parameter values are super imposed over the contour plots as points, which are colored based on the probability of devil persistence for each parameter value.

Alt text for figure 5: Line plots show the changes over time in devil population size, tumor prevalence, and all three devil and tumor trait pairs.

Alt text for figure 6: Violin plots showing the probability of devil persistence (first row) and the probability of devil and devil facial tumor disease coexistence (second row) when different combinations of trait pairs are allowed to coevolve.

Alt text for figure 7: Violin plots showing the proportional devil recovery when different combinations of trait pairs are allowed to coevolve.

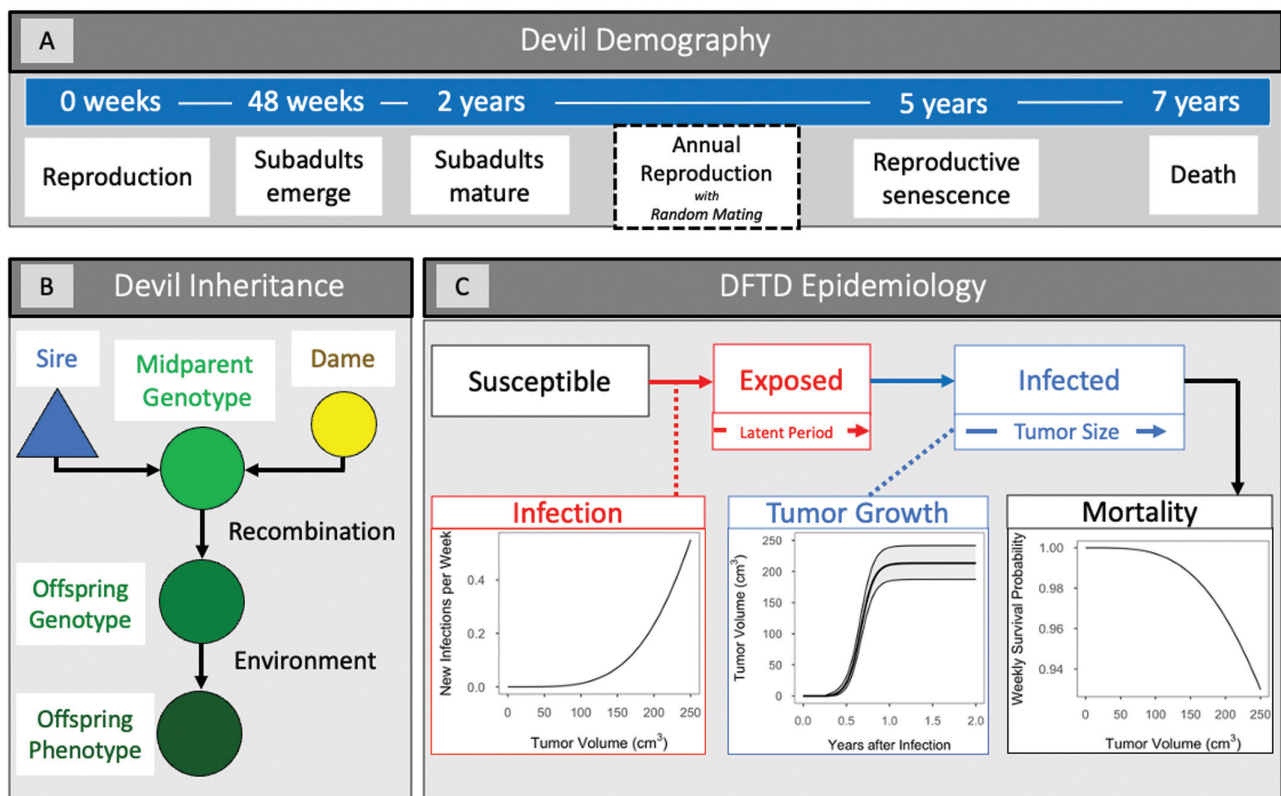


Fig. 1.

DFTD-related Trait Variation

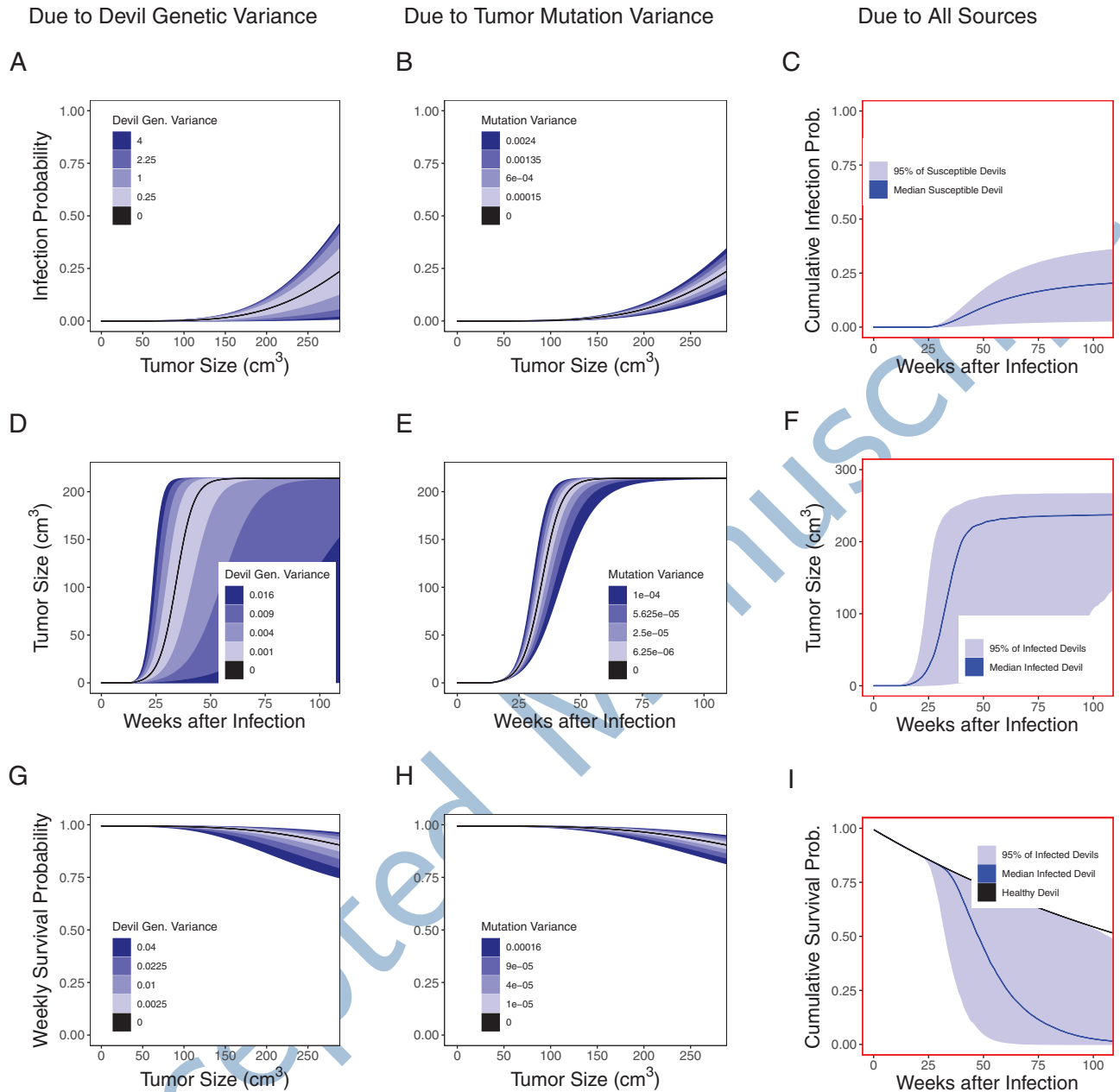


Fig. 2.

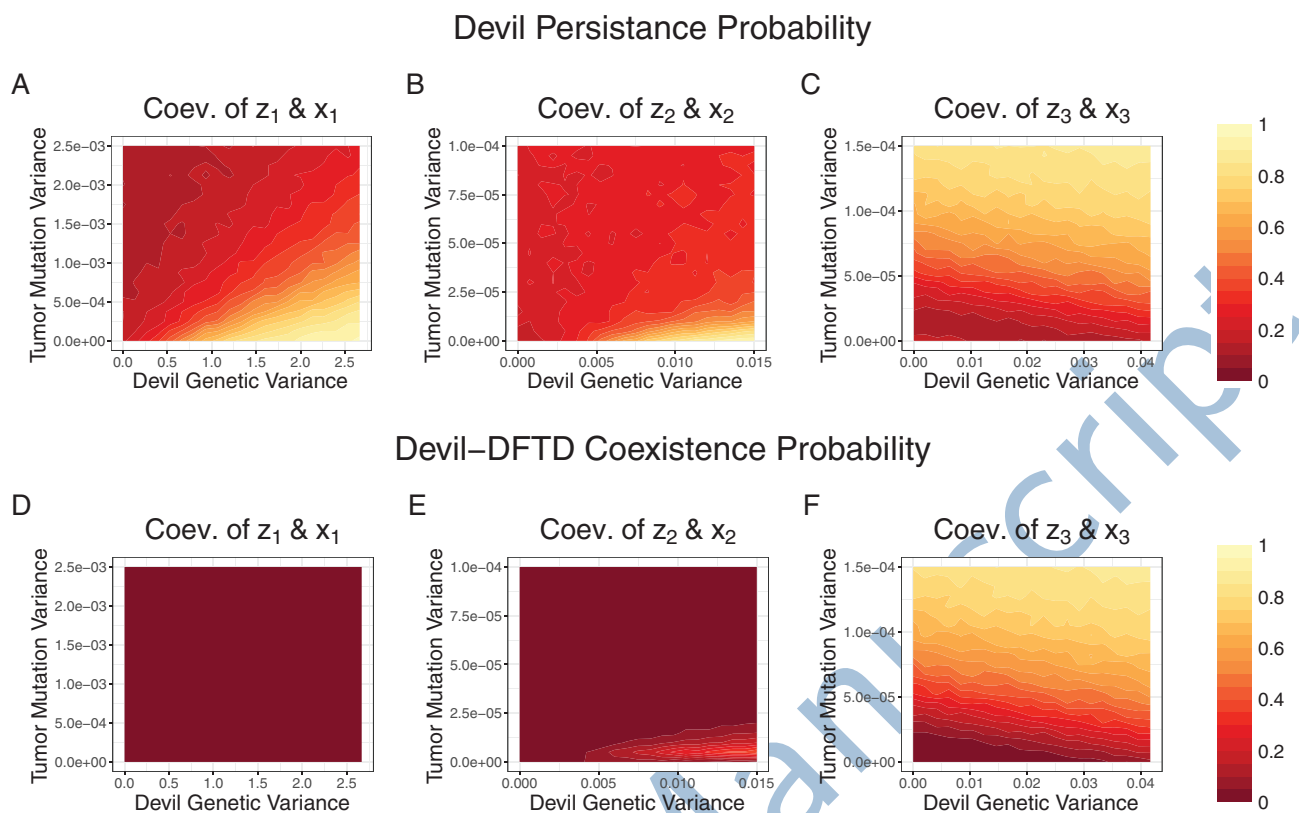


Fig. 3.

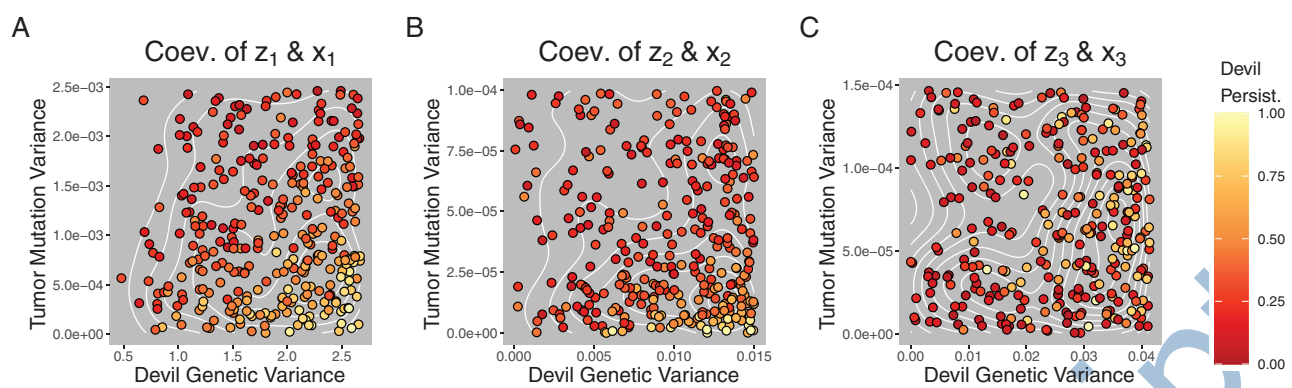


Fig. 4.

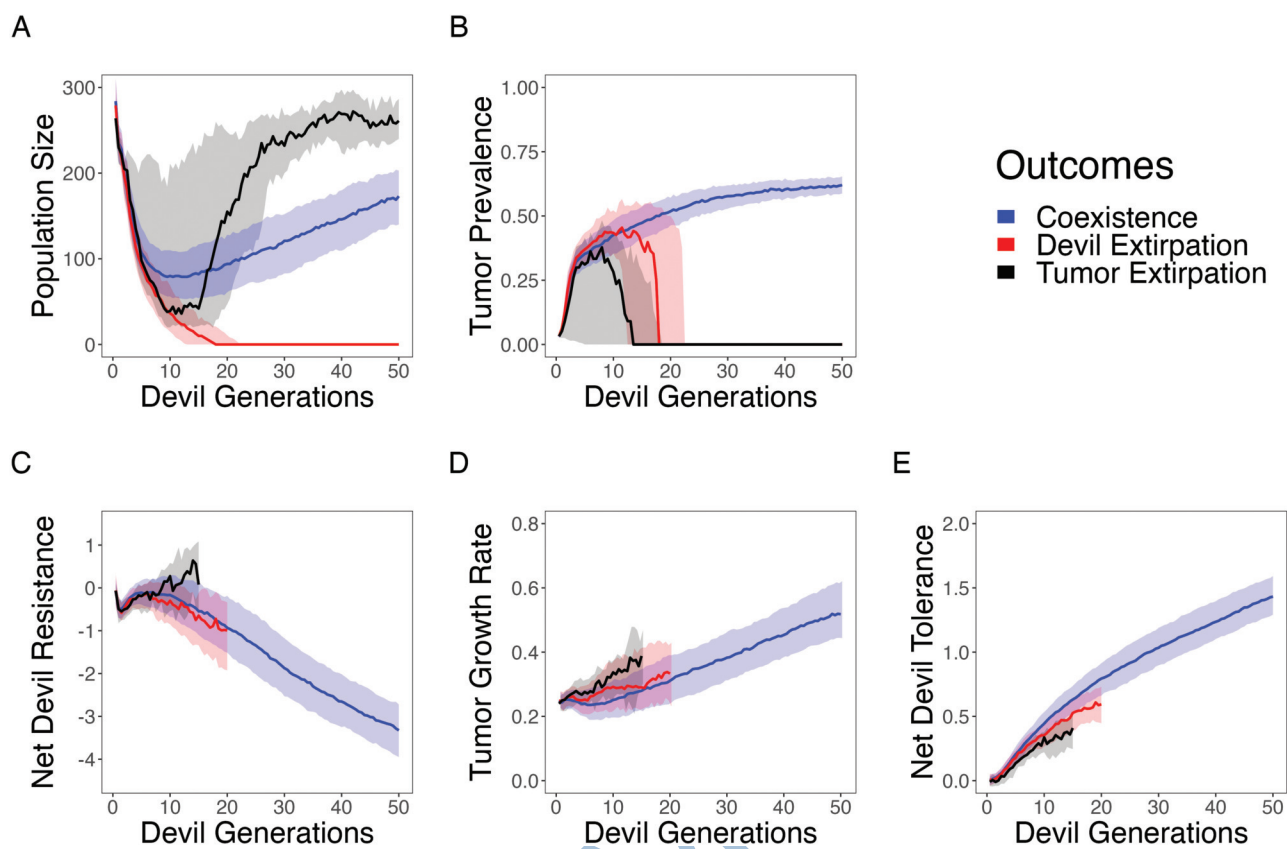


Fig. 5.

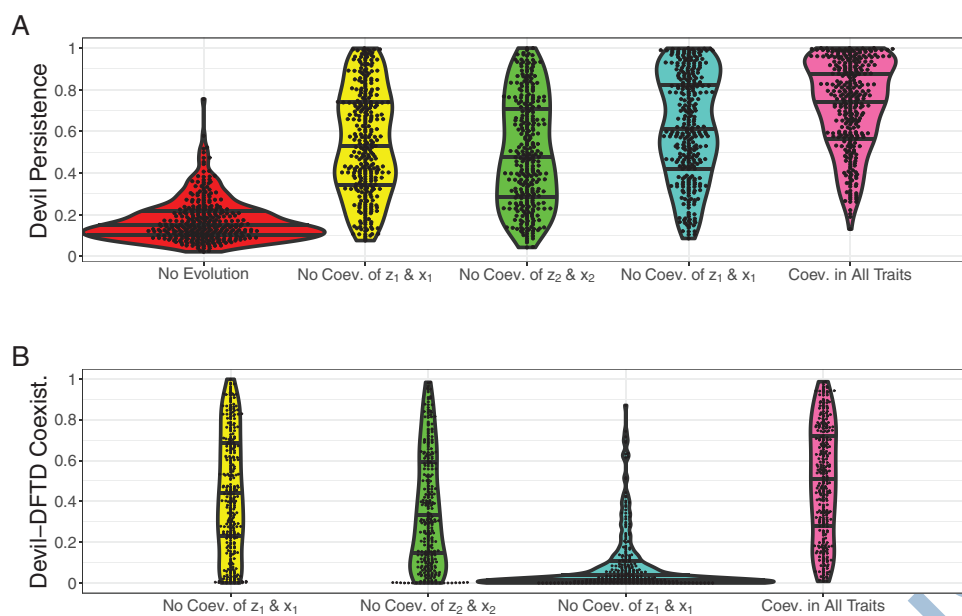


Fig. 6.

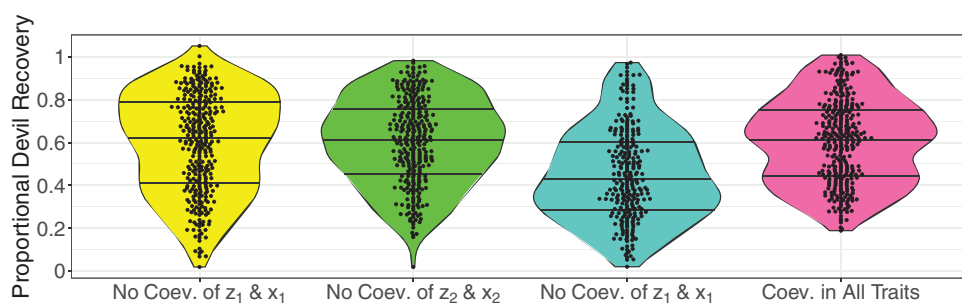


Fig. 7.

Table 1 Names and mathematical notation of the model state variables and the model parameters used in parameter selection. “Realized state variables” are quantities the directly affect individual infection, disease progression, and survival while “latent traits” are the quantitative genetic traits that underlie genetic variation in the realized state variables. Note that the three covariance matrices represent nine, three, and nine, respectively, distinct parameters. See the methods and supplement 2 for the details of the parameter selection process.

Variable Name	Notation	Parameter Name	Notation
<i>Population State Variables</i>		<i>Devil Demographic Parameters</i>	
Time	t	Probability of mating	p_{mate}
Devil population size	N	Offspring survival probability	b_{prob}
Susceptible devils	N_S	Density-dependent death rate	d_{DD}
Infected devils	N_I	Density-independent death rate	d_{DI}
<i>Realized Individual State Variables</i>		Sub-adult excess death rate	d_{SA}
Probability of devil i remaining susceptible	P_i^S	<i>DFTD Parameters</i>	
Realized resistance of devil i to infection by tumor j	R_{ij}	Initial tumor growth rate	r_0^{growth}
Tumor load on devil i	L_i	Tumor growth heterogeneity	λ
Expected tumor load	\bar{L}_i	Maximum tumor load	L_{max}
Time of infection	T_i^I	Tumor latent period	τ
Realized tumor growth rate	r_i^{growth}	Minimum survival probability	S_{min}
Critical tumor size (mortality)	$L_{S,i}^{crit}$	Baseline critical tumor size (mortality)	$L_{S_0}^{crit}$
Devil survival probability	P_i^{surv}	Mortality shape parameter	α
<i>Latent Individual Traits</i>		Maximum Transmission	β
Latent devil resistance to infection	$z_{1,i}$	Critical tumor size (transmission)	L_I^{crit}
Latent devil resistance to tumor growth	$z_{2,i}$	Transmission shape parameter	γ
Latent devil tolerance	$z_{3,i}$	Subadult Resistance Factor	R_{SA}
Devil phenotype vector	\mathbf{z}	<i>Covariance Matrices</i>	
Devil genotype vector	\mathbf{g}	Initial devil genetic covariance matrix	$\mathbf{G}(0)$
Devil genetic covariance matrix	$\mathbf{G}(t)$	Devil environmental covariance matrix	\mathbf{E}
Devil segregation covariance matrix	\mathbf{S}	Tumor mutation covariance matrix	\mathbf{M}
Latent tumor transmissibility	$x_{1,i}$		
Latent tumor growth	$x_{2,i}$		
Latent tumor virulence	$x_{3,i}$		
Tumor phenotype vector	\mathbf{x}		

Table 2 A list of studies used to derive the parameter selection criteria and a brief description of their findings.

Study	Type	Sites Sampled	Sampling Duration	Primary Goal
Lachish et al. 2009	Mark-recapture	Freycinet	1999-2007	Estimate changes in devil age-structure, sex ratio, and breeding behavior due to DFTD.
McCallum et al. 2009	Mark-recapture; SEI model	Fentonbury, Wisedale, Bronte, Buckland, Mt William, Freycinet	1999-2008 (varies by site)	Calculate DFTD R0; Estimates DFTD prevalence and devil density; Predict future DFTD prevalence and devil density
Hamede et al. 2012	Mark-recapture	Fentonbury, Forestier, Freycinet, West Pencil Pine	2001-2010 (varies by site)	Estimate changes in devil density, DFTD prevalence, and devil age-structure due to DFTD
Wells et al. 2017	Bayesian hierarchical mark-recapture model	West Pencil Pine	2006-2015	Estimate tumor growth and the effect of tumor size on devil survival and fecundity
Rose et al. 2017	Review	NA	NA	Review devil ecology, behavior, and reproduction.
Lazenby et al. 2018	Spotlight survey; Mark-recapture	State-wide; Bronte, Buckland, Fentonbury, Granville, Narawntapu, Kempton, Takone, Woolnorth, wukalina	1985 – 2016; 2004-2016 (varies by site)	Estimate changes in devil density, DFTD prevalence, and devil demography due to DFTD
Margres et al. 2018	Genome-wide Association Study (GWAS)	Fentonbury, Forestier, Freycinet, wukalina, Narawntapu, West Pencil Pine	2000-2016 (varies by site)	Estimate contribution of devil genetic variation to variation Case-control, time to infection, and survival after infection
Cunningham et al. 2021	Spatially-explicit mark-recapture; Pattern-oriented diffusion simulation; Bayesian joint-likelihood model	State-wide spotlight surveys; 15 mark-recapture sites (see Cunningham et al. 2021, table S2)	1999-2020 (varies by site)	Estimate and predict state-wide spread of DFTD and changes in devil density
Gallinson et al. 2024	Two-species genome-wide association study (Co-GWAS)	Black River, Freycinet, Takone, West Pencil Pine	2006-2020 (varies by site)	Estimate contribution of devil genetic variation, tumor variation and the interaction of the two to force of infection.

References

- (2008). Tasmanian devil PHVA final report. Technical report, IUCN/SSC Conservation Breeding Specialist Group.
- (2010). Recovery plan for the tasmanian devil (*Sarcophilus harrisii*). Technical report, Department of Primary Industries, Parks, Water and Environment.
- Alizon, S., de Roode, J. C., and Michalakakis, Y. (2013). Multiple infections and the evolution of virulence. *Ecology Letters*, 16(4):556–567.
- Alizon, S., Hurford, A., Mideo, N., and Van Baalen, M. (2009). Virulence evolution and the trade-off hypothesis: history, current state of affairs and the future. *Journal of Evolutionary Biology*, 22(2):245–259.
- Barton, N. H., Etheridge, A. M., and Véber, A. (2017). The infinitesimal model: Definition, derivation, and implications. *Theoretical population biology*, 118:50–73.
- Beeton, N. and McCallum, H. (2011). Models predict that culling is not a feasible strategy to prevent extinction of Tasmanian devils from facial tumour disease. *Journal of Applied Ecology*, 48(6):1315–1323.
- Berngruber, T. W., Lion, S., and Gandon, S. (2013). Evolution of suicide as a defence strategy against pathogens in a spatially structured environment. *Ecology Letters*, 16(4):446–453.
- Bleher, D. S., Hicks, A. C., Behr, M., Meteyer, C. U., Berlowski-Zier, B. M., Buckles, E. L., Coleman, J. T., Darling, S. R., Gargas, A., Niver, R., et al. (2009). Bat white-nose syndrome: an emerging fungal pathogen? *Science*, 323(5911):227–227.
- Bolker, B. M., Nanda, A., and Shah, D. (2010). Transient virulence of emerging pathogens. *Journal of The Royal Society Interface*, 7(46):811–822.
- Boots, M. and Best, A. (2018). The evolution of constitutive and induced defences to infectious disease. *Proceedings of the Royal Society B: Biological Sciences*, 285(1883):20180658.
- Boots, M., Best, A., Miller, M. R., and White, A. (2009). The role of ecological feedbacks in the evolution of host defence: what does theory tell us? *Philosophical Transactions of the Royal Society B: Biological Sciences*, 364(1513):27–36.
- Brannelly, L. A., McCallum, H. I., Grogan, L. F., Briggs, C. J., Ribas, M. P., Hollanders, M., Sasso, T., Familiar López, M., Newell, D. A., and Kilpatrick, A. M. (2021). Mechanisms underlying host persistence following amphibian disease emergence determine appropriate management strategies. *Ecology Letters*, 24(1):130–148.
- Brüniche-Olsen, A., Jones, M. E., Austin, J. J., Burrridge, C. P., and Holland, B. R. (2014). Extensive population decline in the tasmanian devil predates european settlement and devil facial tumour disease. *Biology letters*, 10(11):20140619.
- Brüniche-Olsen, A., Jones, M. E., Burrridge, C. P., Murchison, E. P., Holland, B. R., and Austin, J. J. (2018). Ancient dna tracks the mainland extinction and island survival of the tasmanian devil. *Journal of biogeography*, 45(5):963–976.
- Brüniche-Olsen, A., Austin, J. J., Jones, M. E., Holland, B. R., and Burrridge, C. P. (2016). Detecting Selection on Temporal and Spatial Scales: A Genomic Time-Series Assessment of Selective Responses to Devil Facial Tumor Disease. *PLOS ONE*, 11(3):e0147875.
- Buckingham, L. J. and Ashby, B. (2022). Coevolutionary theory of hosts and parasites. *Journal of Evolutionary Biology*, 35(2):205–224.
- Byrne, A. Q., Vredenburg, V. T., Martel, A., Pasmans, F., Bell, R. C., Blackburn, D. C., Bletz, M. C., Bosch, J., Briggs, C. J., Brown, R. M., Catenazzi, A., Familiar López, M., Figueroa-Valenzuela, R., Ghose, S. L., Jaeger, J. R., Jani, A. J., Jirku, M., Knapp, R. A., Muñoz, A., Portik, D. M., Richards-Zawacki, C. L., Rockney, H., Rovito, S. M., Stark, T., Sulaeman, H., Tao, N. T., Voyles, J., Waddle, A. W., Yuan, Z., and Rosenblum, E. B. (2019). Cryptic diversity of a widespread global pathogen reveals expanded threats to amphibian conservation. *Proceedings of the National Academy of Sciences*, 116(41):20382–20387.
- Carval, D. and Ferriere, R. (2010). A unified model for the coevolution of resistance, tolerance, and virulence: Resistance, tolerance, and virulence. *Evolution*, pages no–no.
- Cheng, Y., Heasman, K., Peck, S., Peel, E., Gooley, R. M., Papenfuss, A. T., Hogg, C. J., and Belov, K. (2017). Significant decline in anticancer immune capacity during puberty in the tasmanian devil. *Scientific Reports*, 7(1):44716.
- Cressler, C. E., McLeod, D. V., Rozins, C., Van Den Hoogen, J., and Day, T. (2016). The adaptive evolution of virulence: a review of theoretical predictions and empirical tests. *Parasitology*, 143(7):915–930.
- Cunningham, C. X., Comte, S., McCallum, H., Hamilton, D. G., Hamede, R. K., Storfer, A., Hollings, T., Ruiz-Aravena, M., Kerlin, D. H., Brook, B. W., Hocking, G., and Jones, M. E. (2021). Quantifying 25 years of disease-caused declines in Tasmanian devil populations: host density drives spatial pathogen spread. *Ecology Letters*, 24(5):958–969.
- De Castro, F. and Bolker, B. M. (2005a). Mechanisms of disease-induced extinction. *Ecology letters*, 8(1):117–126.
- De Castro, F. and Bolker, B. M. (2005b). Parasite establishment and host extinction in model communities. *Oikos*, 111(3):501–513.
- Eddelbuettel, D., Francois, R., Allaire, J., Ushey, K., Kou, Q., Russell, N., Ucar, I., Bates, D., and Chambers, J. (2023). *Rcpp: Seamless R and C++ Integration*. R package version 1.0.11.
- Epstein, B., Jones, M., Hamede, R. K., Hendricks, S., McCallum, H., Murchison, E. P., Schönfeld, B., Wiench, C., Hohenlohe, P., and Storfer, A. (2016). Rapid evolutionary response to a transmissible cancer in Tasmanian devils. *Nature Communications*, 7(1):12684.
- Espejo, C., Wilson, R., Pye, R. J., Ratcliffe, J. C., Ruiz-Aravena, M., Willms, E., Wolfe, B. W., Hamede, R. K., Hill, A. F., Jones, M. E., et al. (2022). Cathelicidin-3 associated with serum extracellular vesicles enables early diagnosis of a transmissible cancer. *Frontiers in Immunology*, 13:858423.
- Fenton, A., Antonovics, J., and Brockhurst, M. A. (2012). Two-step infection processes can lead to coevolution between functionally independent infection and resistance pathways. *Evolution*, 66(7):2030–2041.
- Fisher, M. C., Henk, D. A., Briggs, C. J., Brownstein, J. S., Madoff, L. C., McCraw, S. L., and Gurr, S. J. (2012). Emerging fungal threats to animal, plant and ecosystem health. *Nature*, 484(7393):186–194.

- Fisher, R. A. (1918). Xv.—the correlation between relatives on the supposition of mendelian inheritance. *Earth and Environmental Science Transactions of the Royal Society of Edinburgh*, 52(2):399–433.
- Fraik, A. K., Margres, M. J., Epstein, B., Barbosa, S., Jones, M., Hendricks, S., Schönfeld, B., Stahlke, A. R., Veillet, A., Hamede, R. K., McCallum, H., Lopez-Contreras, E., Kallinen, S. J., Hohenlohe, P. A., Kelley, J. L., and Storfer, A. (2020). Disease swamps molecular signatures of genetic-environmental associations to abiotic factors in Tasmanian devil (*Sarcophilus harrisii*) populations. *Evolution*, 74(7):1392–1408.
- Frankham, R., Bradshaw, C. J., and Brook, B. W. (2014). Genetics in conservation management: revised recommendations for the 50/500 rules, red list criteria and population viability analyses. *Biological Conservation*, 170:56–63.
- Gallinson, D. G., Kozakiewicz, C. P., Rautsaw, R. M., Beer, M. A., Ruiz-Aravena, M., Compère, S., Hamilton, D. G., Kerlin, D. H., McCallum, H., Hamede, R. K., Jones, M. E., Storfer, A., McMinds, R., and Margres, M. J. (2024). Intergenomic signatures of coevolution between tasmanian devils and an infectious cancer. *Proceedings of the National Academy of Sciences*, 121(12):e2307780121.
- Gilchrist, M. A. and Sasaki, A. (2002). Modeling Host–Parasite Coevolution: A Nested Approach Based on Mechanistic Models. *Journal of Theoretical Biology*, 218(3):289–308.
- Glasscock, G. L., Grueber, C. E., Belov, K., and Hogg, C. J. (2021). Reducing the Extinction Risk of Populations Threatened by Infectious Diseases. *Diversity*, 13(2):63.
- Gomulkiewicz, R., Holt, R. D., Barfield, M., and Nuismer, S. L. (2010). Genetics, adaptation, and invasion in harsh environments. *Evolutionary Applications*, 3(2):97–108.
- Gooley, R. M., Hogg, C. J., Fox, S., Pemberton, D., Belov, K., and Grueber, C. E. (2020). Inbreeding depression in one of the last DFTD-free wild populations of Tasmanian devils. *PeerJ*, 8:e9220.
- Grimm, V., Berger, U., Bastiansen, F., Eliassen, S., Ginot, V., Giske, J., Goss-Custard, J., Grand, T., Heinz, S. K., Huse, G., et al. (2006). A standard protocol for describing individual-based and agent-based models. *Ecological modelling*, 198(1-2):115–126.
- Grimm, V., Berger, U., DeAngelis, D. L., Polhill, J. G., Giske, J., and Railsback, S. F. (2010). The odd protocol: a review and first update. *Ecological modelling*, 221(23):2760–2768.
- Grimm, V., Railsback, S. F., Vincenot, C. E., Berger, U., Gallagher, C., DeAngelis, D. L., Edmonds, B., Ge, J., Giske, J., Groeneveld, J., et al. (2020). The odd protocol for describing agent-based and other simulation models: A second update to improve clarity, replication, and structural realism. *Journal of Artificial Societies and Social Simulation*, 23(2).
- Grogan, L. F., Mangan, M. J., and McCallum, H. I. (2023). Amphibian infection tolerance to chytridiomycosis. *Philosophical Transactions of the Royal Society B: Biological Sciences*, 378(1882):20220133.
- Grueber, C. E., Fox, S., McLennan, E. A., Gooley, R. M., Pemberton, D., Hogg, C. J., and Belov, K. (2019). Complex problems need detailed solutions: Harnessing multiple data types to inform genetic management in the wild. *Evolutionary Applications*, 12(2):280–291.
- Hairton, N. G., Ellner, S. P., Geber, M. A., Yoshida, T., and Fox, J. A. (2005). Rapid evolution and the convergence of ecological and evolutionary time. *Ecology Letters*, 8(10):1114–1127.
- Hall, M. D., Bento, G., and Ebert, D. (2017). The Evolutionary Consequences of Stepwise Infection Processes. *Trends in Ecology & Evolution*, 32(8):612–623.
- Hamede, R. K., Beeton, N. J., Carver, S., and Jones, M. E. (2017). Untangling the model muddle: empirical tumour growth in tasmanian devil facial tumour disease. *Scientific Reports*, 7(1):6217.
- Hamede, R. K., Fountain-Jones, N. M., Arce, F., Jones, M., Storfer, A., Hohenlohe, P. A., McCallum, H., Roche, B., Ujvari, B., and Thomas, F. (2023). The tumour is in the detail: Local phylogenetic, population and epidemiological dynamics of a transmissible cancer in Tasmanian devils. *Evolutionary Applications*, 16(7):1316–1327.
- Hamede, R. K., Lachish, S., Belov, K., Woods, G., Kreiss, A., Pearce, A., Lazenby, B., Jones, M., and McCallum, H. (2012). Reduced Effect of Tasmanian Devil Facial Tumor Disease at the Disease Front. *Conservation Biology*, 26(1):124–134.
- Hamede, R. K., Madsen, T., McCallum, H., Storfer, A., Hohenlohe, P. A., Siddle, H., Kaufman, J., Giraudeau, M., Jones, M., Thomas, F., and Ujvari, B. (2021). Darwin, the devil, and the management of transmissible cancers. *Conservation Biology*, 35(2):748–751.
- Hamede, R. K., McCallum, H., and Jones, M. (2008). Seasonal, demographic and density-related patterns of contact between Tasmanian devils (*Sarcophilus harrisii*): Implications for transmission of devil facial tumour disease. *Austral Ecology*, 33(5):614–622.
- Hamede, R. K., McCallum, H., and Jones, M. (2013). Biting injuries and transmission of Tasmanian devil facial tumour disease. *Journal of Animal Ecology*, 82(1):182–190.
- Hamilton, D. G., Jones, M. E., Cameron, E. Z., Kerlin, D. H., McCallum, H., Storfer, A., Hohenlohe, P. A., and Hamede, R. K. (2020). Infectious disease and sickness behaviour: tumour progression affects interaction patterns and social network structure in wild Tasmanian devils. *Proceedings of the Royal Society B: Biological Sciences*, 287(1940):20202454.
- Hamilton, D. G., Jones, M. E., Cameron, E. Z., McCallum, H., Storfer, A., Hohenlohe, P. A., and Hamede, R. K. (2019). Rate of intersexual interactions affects injury likelihood in Tasmanian devil contact networks. *Behavioral Ecology*, 30(4):1087–1095.
- Handel, A. and Rohani, P. (2015). Crossing the scale from within-host infection dynamics to between-host transmission fitness: a discussion of current assumptions and knowledge. *Philosophical Transactions of the Royal Society B: Biological Sciences*, 370(1675):20140302.
- Hedrick, P. W. and Garcia-Dorado, A. (2016). Understanding inbreeding depression, purging, and genetic rescue. *Trends in ecology & evolution*, 31(12):940–952.
- Hendricks, S., Epstein, B., Schönfeld, B., Wiench, C., Hamede, R. K., Jones, M., Storfer, A., and Hohenlohe, P. (2017). Conservation implications of limited genetic diversity and population structure in Tasmanian devils (*Sarcophilus harrisii*). *Conservation Genetics*, 18(4):977–982.

- Hendry, A. P. and Gonzalez, A. (2008). Whither adaptation? *Biology & Philosophy*, 23(5):673–699.
- Hendry, A. P., Schoen, D. J., Wolak, M. E., and Reid, J. M. (2018). The Contemporary Evolution of Fitness. *Annual Review of Ecology, Evolution, and Systematics*, 49(1):457–476.
- Hesterman, H. (2008). *Reproductive physiology of the Tasmanian devil (Sarcophilus harrisii) and spotted-tailed quail (Dasyurus maculatus)*. Dissertation, University of Tasmania.
- Hesterman, H., Jones, S., and Schwarzenberger, F. (2008). Reproductive endocrinology of the largest dasyurids: Characterization of ovarian cycles by plasma and fecal steroid monitoring. part i. the tasmanian devil (*sarcophilus harrisii*). *General and Comparative Endocrinology*, 155(1):234–244.
- Hogg, C., Lee, A., Srb, C., and Hibbard, C. (2017). Metapopulation management of an endangered species with limited genetic diversity in the presence of disease: the tasmanian devil *sarcophilus harrisii*. *International Zoo Yearbook*, 51(1):137–153.
- Hogg, C. J., Ivy, J. A., Srb, C., Hockley, J., Lees, C., Hibbard, C., and Jones, M. (2015). Influence of genetic provenance and birth origin on productivity of the tasmanian devil insurance population. *Conservation Genetics*, 16:1465–1473.
- Hohenlohe, P. A., McCallum, H. I., Jones, M. E., Lawrence, M. F., Hamede, R. K., and Storfer, A. (2019). Conserving adaptive potential: lessons from Tasmanian devils and their transmissible cancer. *Conservation Genetics*, 20(1):81–87.
- Hoyt, J. R., Kilpatrick, A. M., and Langwig, K. E. (2021). Ecology and impacts of white-nose syndrome on bats. *Nature Reviews Microbiology*, 19(3):196–210.
- Hubert, J.-N., Zerjal, T., and Hospital, F. (2018). Cancer- and behavior-related genes are targeted by selection in the Tasmanian devil (*Sarcophilus harrisii*). *PLOS ONE*, 13(8):e0201838.
- James, S., Jennings, G., Kwon, Y. M., Stammnitz, M., Fraik, A., Storfer, A., Comte, S., Pemberton, D., Fox, S., Brown, B., Pye, R., Woods, G., Lyons, B., Hohenlohe, P. A., McCallum, H., Siddle, H., Thomas, F., Ujvari, B., Murchison, E. P., Jones, M., and Hamede, R. K. (2019). Tracing the rise of malignant cell lines: Distribution, epidemiology and evolutionary interactions of two transmissible cancers in Tasmanian devils. *Evolutionary Applications*, 12(9):1772–1780.
- Jones, M. E., Cockburn, A., Hamede, R. K., Hawkins, C., Hesterman, H., Lachish, S., Mann, D., McCallum, H., and Pemberton, D. (2008). Life-history change in disease-ravaged Tasmanian devil populations. *Proceedings of the National Academy of Sciences*, 105(29):10023–10027.
- Kamiya, T., Oña, L., Wertheim, B., and van Doorn, G. S. (2016). Coevolutionary feedback elevates constitutive immune defence: a protein network model. *BMC Evolutionary Biology*, 16:1–10.
- Kerr, P. J. (2012). Myxomatosis in australia and europe: a model for emerging infectious diseases. *Antiviral research*, 93(3):387–415.
- Kerr, P. J., Cattadori, I. M., Liu, J., Sim, D. G., Dodds, J. W., Brooks, J. W., Kennett, M. J., Holmes, E. C., and Read, A. F. (2017). Next step in the ongoing arms race between myxoma virus and wild rabbits in australia is a novel disease phenotype. *Proceedings of the National Academy of Sciences*, 114(35):9397–9402.
- Kerr, P. J., Cattadori, I. M., Sim, D., Liu, J., Holmes, E. C., and Read, A. F. (2022). Divergent evolutionary pathways of myxoma virus in australia: virulence phenotypes in susceptible and partially resistant rabbits indicate possible selection for transmissibility. *Journal of virology*, 96(20):e00886–22.
- Kwon, Y. M., Gori, K., Park, N., Potts, N., Swift, K., Wang, J., Stammnitz, M. R., Cannell, N., Baez-Ortega, A., Comte, S., Fox, S., Harmsen, C., Huxtable, S., Jones, M., Kreiss, A., Lawrence, C., Lazenby, B., Peck, S., Pye, R., Woods, G., Zimmermann, M., Wedge, D. C., Pemberton, D., Stratton, M. R., Hamede, R. K., and Murchison, E. P. (2020). Evolution and lineage dynamics of a transmissible cancer in Tasmanian devils. *PLOS Biology*, 18(11):e3000926.
- Lachish, S., McCallum, H., and Jones, M. (2009). Demography, disease and the devil: life-history changes in a disease-affected population of Tasmanian devils (*Sarcophilus harrisii*). *Journal of Animal Ecology*, 78(2):427–436.
- Lachish, S., Miller, K., Storfer, A., Goldizen, A., and Jones, M. (2011). Evidence that disease-induced population decline changes genetic structure and alters dispersal patterns in the tasmanian devil. *Heredity*, 106(1):172–182.
- Langwig, K. E., Hoyt, J. R., Parise, K. L., Frick, W. F., Foster, J. T., and Kilpatrick, A. M. (2017). Resistance in persisting bat populations after white-nose syndrome invasion. *Philosophical Transactions of the Royal Society B: Biological Sciences*, 372(1712):20160044.
- Lazenby, B. T., Tobler, M. W., Brown, W. E., Hawkins, C. E., Hocking, G. J., Hume, F., Huxtable, S., Iles, P., Jones, M. E., Lawrence, C., Thalmann, S., Wise, P., Williams, H., Fox, S., and Pemberton, D. (2018). Density trends and demographic signals uncover the long-term impact of transmissible cancer in Tasmanian devils. *Journal of Applied Ecology*, 55(3):1368–1379.
- Leathlobhair, M. N. and Lenski, R. E. (2022). Population genetics of clonally transmissible cancers. *Nature Ecology & Evolution*, 6(8):1077–1089.
- Lips, K. R., Brem, F., Brenes, R., Reeve, J. D., Alford, R. A., Voyles, J., Carey, C., Livo, L., Pessier, A. P., and Collins, J. P. (2006). Emerging infectious disease and the loss of biodiversity in a neotropical amphibian community. *Proceedings of the National Academy of Sciences*, 103(9):3165–3170.
- Lively, C. M. (2010). An epidemiological model of host-parasite coevolution and sex: Epidemiological model of host-parasite coevolution and sex. *Journal of Evolutionary Biology*, 23(7):1490–1497.
- Lively, C. M. (2016). Coevolutionary Epidemiology: Disease Spread, Local Adaptation, and Sex. *The American Naturalist*, 187(3):E77–E82.
- Luque, G. M., Vayssade, C., Facon, B., Guillemaud, T., Courchamp, F., and Fauvergue, X. (2016). The genetic allee effect: a unified framework for the genetics and demography of small populations. *Ecosphere*, 7(7):e01413.
- Margres, M. J., Jones, M. E., Epstein, B., Kerlin, D. H., Comte, S., Fox, S., Fraik, A. K., Hendricks, S. A., Huxtable, S., Lachish, S., Lazenby, B., O'Rourke, S. M., Stahlke, A. R., Wiench, C. G., Hamede, R. K., Schönfeld, B., McCallum, H., Miller, M. R., Hohenlohe, P. A., and Storfer, A. (2018). Large-effect loci affect survival in Tasmanian devils (*Sarcophilus harrisii*) infected with a transmissible cancer. *Molecular Ecology*, 27(21):4189–4199.

- Margres, M. J., Ruiz-Aravena, M., Hamede, R. K., Chawla, K., Patton, A. H., Lawrance, M. F., Fraik, A. K., Stahlke, A. R., Davis, B. W., Ostrander, E. A., Jones, M. E., McCallum, H., Paddison, P. J., Hohenlohe, P. A., Hockenbery, D., and Storfer, A. (2020). Spontaneous Tumor Regression in Tasmanian Devils Associated with *RASL11A* Activation. *Genetics*, 215(4):1143–1152.
- McCallum, H., Barlow, N., and Hone, J. (2001). How should pathogen transmission be modelled? *Trends in ecology & evolution*, 16(6):295–300.
- McCallum, H., Fenton, A., Hudson, P. J., Lee, B., Levick, B., Norman, R., Perkins, S. E., Viney, M., Wilson, A. J., and Lello, J. (2017). Breaking beta: deconstructing the parasite transmission function. *Philosophical Transactions of the Royal Society B: Biological Sciences*, 372(1719):20160084.
- McCallum, H., Jones, M., Hawkins, C., Hamede, R. K., Lachish, S., Sinn, D. L., Beeton, N., and Lazenby, B. (2009). Transmission dynamics of Tasmanian devil facial tumor disease may lead to disease-induced extinction. *Ecology*, 90(12):3379–3392.
- McKnight, D. T., Schwarzkopf, L., Alford, R. A., Bower, D. S., and Zenger, K. R. (2017). Effects of emerging infectious diseases on host population genetics: a review. *Conservation Genetics*, 18(6):1235–1245.
- McLennan, E. A., Gooley, R. M., Wise, P., Belov, K., Hogg, C. J., and Grueber, C. E. (2018). Pedigree reconstruction using molecular data reveals an early warning sign of gene diversity loss in an island population of Tasmanian devils (*Sarcophilus harrisii*). *Conservation Genetics*, 19(2):439–450.
- Miller, W., Hayes, V. M., Ratan, A., Petersen, D. C., Wittekindt, N. E., Miller, J., Walenz, B., Knight, J., Qi, J., Zhao, F., Wang, Q., Bedoya-Reina, O. C., Katiyar, N., Tomsho, L. P., Kasson, L. M., Hardie, R.-A., Woodbridge, P., Tindall, E. A., Bertelsen, M. F., Dixon, D., Pyecroft, S., Helgen, K. M., Lesk, A. M., Pringle, T. H., Patterson, N., Zhang, Y., Kreiss, A., Woods, G. M., Jones, M. E., and Schuster, S. C. (2011). Genetic diversity and population structure of the endangered marsupial *Sarcophilus harrisii* (Tasmanian devil). *Proceedings of the National Academy of Sciences*, 108(30):12348–12353.
- Nuismer, S. L. (2017). *Introduction to coevolutionary theory*. Macmillan Higher Education.
- Nuismer, S. L. and Dybdahl, M. F. (2016). Quantifying the coevolutionary potential of multistep immune defenses. *Evolution*, 70(2):282–295.
- Núñez-Farfán, J., Fornoni, J., and Valverde, P. L. (2007). The Evolution of Resistance and Tolerance to Herbivores. *Annual Review of Ecology, Evolution, and Systematics*, 38(1):541–566.
- Patton, A. H., Lawrance, M. F., Margres, M. J., Kozakiewicz, C. P., Hamede, R. K., Ruiz-Aravena, M., Hamilton, D. G., Comte, S., Ricci, L. E., Taylor, R. L., Stadler, T., Leaché, A., McCallum, H., Jones, M. E., Hohenlohe, P. A., and Storfer, A. (2020). A transmissible cancer shifts from emergence to endemism in Tasmanian devils. *Science*, 370(6522):eabb9772.
- Pemberton, D. (1990). *Social organisation and behaviour of the Tasmanian devil, Sarcophilus harrisii*. Dissertation, University of Tasmania.
- Post, D. M. and Palkovacs, E. P. (2009). Eco-evolutionary feedbacks in community and ecosystem ecology: interactions between the ecological theatre and the evolutionary play. *Philosophical Transactions of the Royal Society B: Biological Sciences*, 364(1523):1629–1640.
- Pyecroft, S. B., Pearse, A.-M., Loh, R., Swift, K., Belov, K., Fox, N., Noonan, E., Hayes, D., Hyatt, A., Wang, L., et al. (2007). Towards a case definition for devil facial tumour disease: what is it? *EcoHealth*, 4:346–351.
- R Core Team (2023). *R: A Language and Environment for Statistical Computing*. R Foundation for Statistical Computing, Vienna, Austria.
- Restif, O. and Koella, J. C. (2004). Concurrent Evolution of Resistance and Tolerance to Pathogens. *The American Naturalist*, 164(4):E90–E102.
- Reznick, D. N., Losos, J., and Travis, J. (2019). From low to high gear: there has been a paradigm shift in our understanding of evolution. *Ecology Letters*, 22(2):233–244.
- Rose, R. K., Pemberton, D. A., Mooney, N. J., and Jones, M. E. (2017). *Sarcophilus harrisii* (Dasyuromorphia: Dasyuridae). *Mammalian Species*, 49(942):1–17.
- Roy, B. A. and Kirchner, J. W. (2000). Evolutionary dynamics of pathogen resistance and tolerance. *Evolution*, 54(1):51–63.
- Ruiz-Aravena, M., Jones, M. E., Carver, S., Estay, S., Espejo, C., Storfer, A., and Hamede, R. K. (2018). Sex bias in ability to cope with cancer: Tasmanian devils and facial tumour disease. *Proceedings of the Royal Society B*, 285(1891):20182239.
- Russell, T., Lane, A., Clarke, J., Hogg, C., Morris, K., Keeley, T., Madsen, T., and Ujvari, B. (2019). Multiple paternity and precocial breeding in wild tasmanian devils, *sarcophilus harrisii* (marsupialia: Dasyuridae). *Biological Journal of the Linnean Society*, 128(1):201–210.
- Råberg, L., Graham, A. L., and Read, A. F. (2009). Decomposing health: tolerance and resistance to parasites in animals. *Philosophical Transactions of the Royal Society B: Biological Sciences*, 364(1513):37–49.
- Råberg, L., Sim, D., and Read, A. F. (2007). Disentangling Genetic Variation for Resistance and Tolerance to Infectious Diseases in Animals. *Science*, 318(5851):812–814.
- Saunders, G., Cooke, B., McColl, K., Shine, R., and Peacock, T. (2010). Modern approaches for the biological control of vertebrate pests: an australian perspective. *Biological control*, 52(3):288–295.
- Schoener, T. W. (2011). The Newest Synthesis: Understanding the Interplay of Evolutionary and Ecological Dynamics. *Science*, 331(6016):426–429.
- Searle, C. L. and Christie, M. R. (2021). Evolutionary rescue in host-pathogen systems*. *Evolution*, 75(11):2948–2958.
- Shefferson, R. P., Mason, C. M., Kellett, K. M., Goolsby, E. W., Coughlin, E., and Flynn, R. W. (2018). The evolutionary impacts of conservation actions. *Population Ecology*, 60(1-2):49–59.
- Shin, J. and MacCarthy, T. (2016). Potential for evolution of complex defense strategies in a multi-scale model of virus-host coevolution. *BMC Evolutionary Biology*, 16:1–15.
- Singh, P. and Best, A. (2021). Simultaneous evolution of host resistance and tolerance to parasitism. *Journal of Evolutionary Biology*, 34(12):1932–1943.

- Siska, V., Eriksson, A., Mehlig, B., and Manica, A. (2018). A metapopulation model of the spread of the devil facial tumour disease predicts the long term collapse of its host but not its extinction. *bioRxiv*.
- Smith, T. B., Kinnison, M. T., Strauss, S. Y., Fuller, T. L., and Carroll, S. P. (2014). Prescriptive Evolution to Conserve and Manage Biodiversity. *Annual Review of Ecology, Evolution, and Systematics*, 45(1):1–22.
- Stahlke, A. R., Epstein, B., Barbosa, S., Margres, M. J., Patton, A. H., Hendricks, S. A., Veillet, A., Fraik, A. K., Schönfeld, B., McCallum, H. I., Hamede, R. K., Jones, M. E., Storfer, A., and Hohenlohe, P. A. (2021). Contemporary and historical selection in Tasmanian devils (*Sarcophilus harrisii*) support novel, polygenic response to transmissible cancer. *Proceedings of the Royal Society B: Biological Sciences*, 288(1951):20210577.
- Stammnitz, M. R., Gori, K., Kwon, Y. M., Harry, E., Martin, F. J., Billis, K., Cheng, Y., Baez-Ortega, A., Chow, W., Comte, S., Eggertsson, H., Fox, S., Hamede, R. K., Jones, M., Lazenby, B., Peck, S., Pye, R., Quail, M. A., Swift, K., Wang, J., Wood, J., Howe, K., Stratton, M. R., Ning, Z., and Murchison, E. P. (2023). The evolution of two transmissible cancers in Tasmanian devils. *Science*, 380(6642):283–293.
- Storfer, A., Epstein, B., Jones, M., Micheletti, S., Spear, S. F., Lachish, S., and Fox, S. (2017). Landscape genetics of the Tasmanian devil: implications for spread of an infectious cancer. *Conservation Genetics*, 18(6):1287–1297.
- Storfer, A., Hohenlohe, P. A., Margres, M. J., Patton, A., Fraik, A. K., Lawrance, M., Ricci, L. E., Stahlke, A. R., McCallum, H. I., and Jones, M. E. (2018). The devil is in the details: Genomics of transmissible cancers in Tasmanian devils. *PLOS Pathogens*, 14(8):e1007098.
- Strickland, K., Jones, M., Storfer, A., Hamede, R., Hohenlohe, P., Margres, M., McCallum, H., Comte, S., Lachish, S., and Kruuk, L. E. (2024). Adaptive potential in the face of a transmissible cancer in tasmanian devils. *EcoEvoRxiv*.
- Stroustrup, B. (2013). *The C++ programming language*. Pearson Education.
- Valenzuela-Sánchez, A., Schmidt, B. R., Uribe-Rivera, D. E., Costas, F., Cunningham, A. A., and Soto-Azat, C. (2017). Cryptic disease-induced mortality may cause host extinction in an apparently stable host–parasite system. *Proceedings of the Royal Society B: Biological Sciences*, 284(1863):20171176.
- Vander Wal, E., Garant, D., Calmé, S., Chapman, C. A., Festa-Bianchet, M., Millien, V., Rioux-Paquette, S., and Pelletier, F. (2014a). Applying evolutionary concepts to wildlife disease ecology and management. *Evolutionary Applications*, 7(7):856–868.
- Vander Wal, E., Garant, D., and Pelletier, F. (2014b). Evolutionary perspectives on wildlife disease: concepts and applications. *Evolutionary Applications*, 7(7):715–722.
- Voyles, J., Woodhams, D. C., Saenz, V., Byrne, A. Q., Perez, R., Rios-Sotelo, G., Ryan, M. J., Bletz, M. C., Sobell, F. A., McLetchie, S., et al. (2018). Shifts in disease dynamics in a tropical amphibian assemblage are not due to pathogen attenuation. *Science*, 359(6383):1517–1519.
- Voyles, J., Young, S., Berger, L., Campbell, C., Voyles, W. F., Dinudom, A., Cook, D., Webb, R., Alford, R. A., Skerratt, L. F., and Speare, R. (2009). Pathogenesis of Chytridiomycosis, a Cause of Catastrophic Amphibian Declines. *Science*, 326(5952):582–585.
- Vredenburg, V. T., Knapp, R. A., Tunstall, T. S., and Briggs, C. J. (2010). Dynamics of an emerging disease drive large-scale amphibian population extinctions. *Proceedings of the National Academy of Sciences*, 107(21):9689–9694.
- Walsh, B. and Lynch, M. (2018). *Evolution and selection of quantitative traits*. Oxford University Press.
- Wells, K., Hamede, R. K., Jones, M. E., Hohenlohe, P. A., Storfer, A., and McCallum, H. I. (2019). Individual and temporal variation in pathogen load predicts long-term impacts of an emerging infectious disease. *Ecology*, 100(3):e02613.
- Wells, K., Hamede, R. K., Kerlin, D. H., Storfer, A., Hohenlohe, P. A., Jones, M. E., and McCallum, H. I. (2017). Infection of the fittest: devil facial tumour disease has greatest effect on individuals with highest reproductive output. *Ecology Letters*, 20(6):770–778.
- Whiteley, A. R., Fitzpatrick, S. W., Funk, W. C., and Tallmon, D. A. (2015). Genetic rescue to the rescue. *Trends in ecology & evolution*, 30(1):42–49.
- Wilber, M. Q., DeMarchi, J. A., Briggs, C. J., and Streipert, S. (2024). Rapid evolution of resistance and tolerance leads to variable host recoveries following disease-induced declines. *The American Naturalist*, 203(5):1160–1181.
- Wilber, M. Q., Knapp, R. A., Toothman, M., and Briggs, C. J. (2017). Resistance, tolerance and environmental transmission dynamics determine host extinction risk in a load-dependent amphibian disease. *Ecology Letters*, 20(9):1169–1181.
- Yamamichi, M. and Ellner, S. P. (2016). Antagonistic coevolution between quantitative and mendelian traits. *Proceedings of the Royal Society B: Biological Sciences*, 283(1827):20152926.